



De-embedding Techniques for Evaluation of Die-Die Interconnect structure on the Interposer Technology

Interconnect Course Project

Milad Seyedi

Course professor: Dr. Nasser Masoumi

Teacher Assistant: Pouya Namaki

28.4.1400

□ Introduction

□ Cascade Based De-embedding

- TRL Method
- 2X Thru Method
- 1X Fixture Method

□ Lumped Equivalent Circuit Model Based

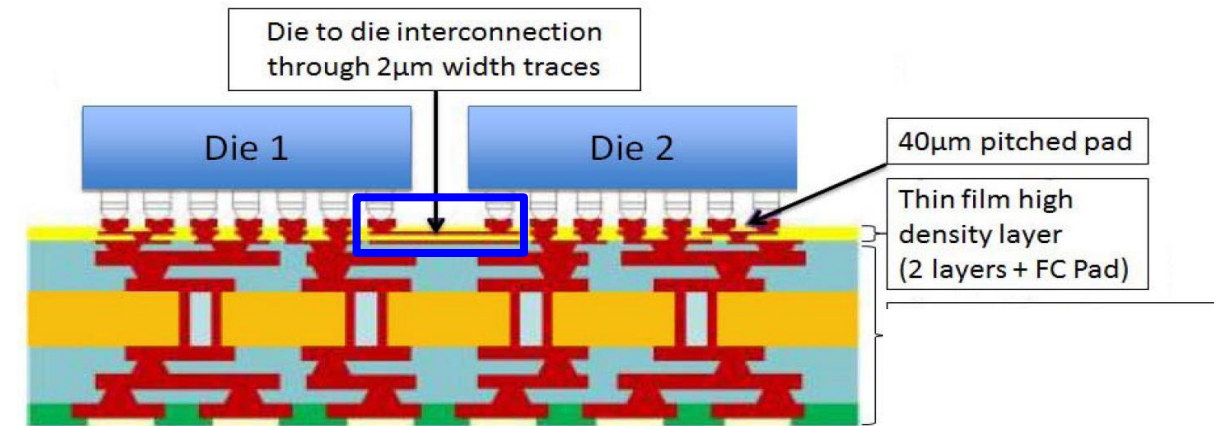
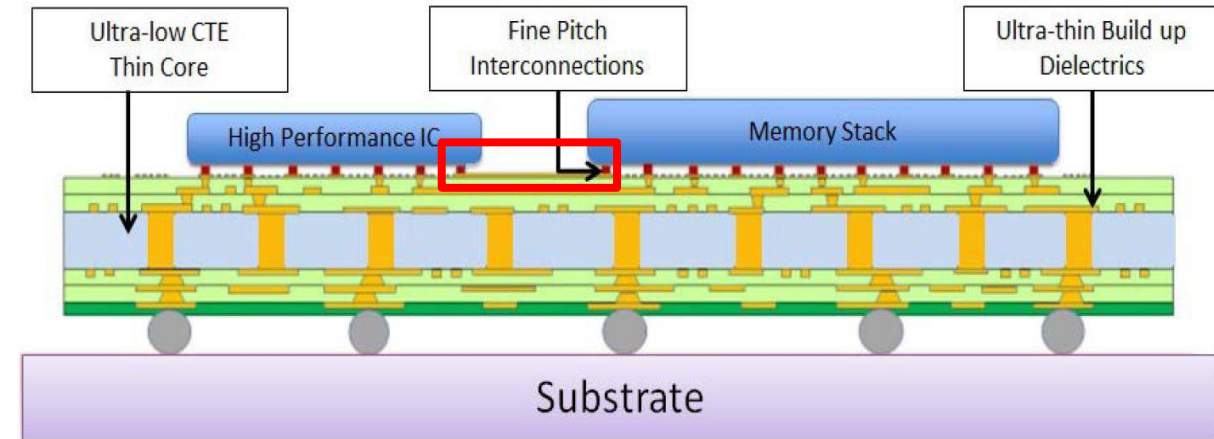
- $L_i L_j$ Method
- Hybrid Method
- **L-2L Method**
 - Use L-2L method form large line's length (PCB Trace + Bump)
 - Electromagnetic Characteristics of Multiport TSVs Using L-2L De-Embedding Method and Shielding TSVs

□ Conclusion

Introduction

3

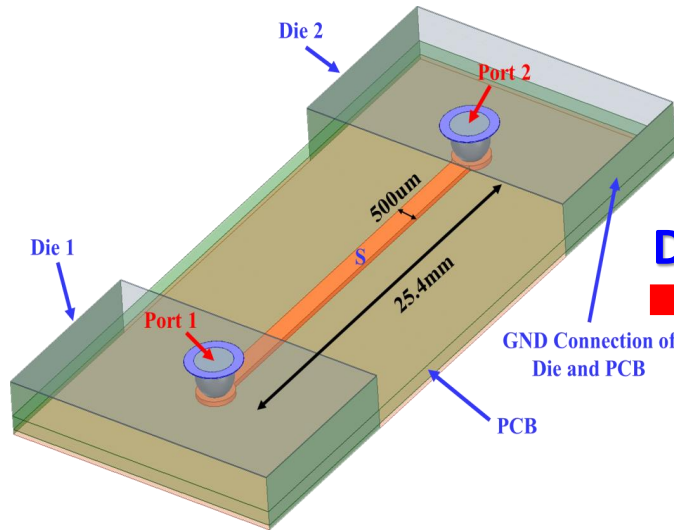
- ❖ An “**interposer**” is an electrical interface (substrate) used for routing between one socket or connection to another socket or connection.
- ❖ In the search for **low-cost interposer technology**, **organic** is one promising candidate. It is typically manufactured by the conventional wet etching process.
- ❖ The **minimum line and spacing of 2 μm** has been achieved in the **traditional organic** multichip package.
- ❖ when a chip is mounted on an organic interposer, either using **wire-bonding** or **flip-chip** technique, the **solder balls** on the package will give some stand-off to the component that will result in **improved reliability**.



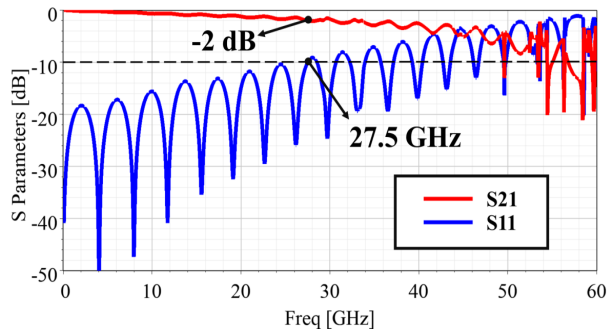
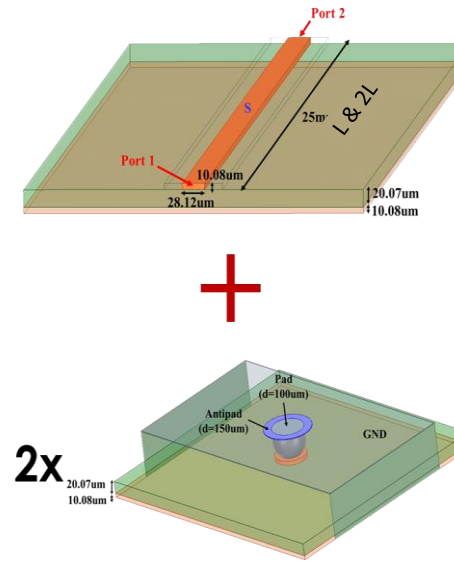
Ref: Interposer Technologies for High-Performance Applications IEEE TRANSACTIONS ON COMPONENTS, PACKAGING AND MANUFACTURING TECHNOLOGY, 2017

De-embedding Technique

4

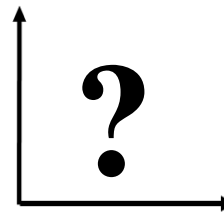


De-embedding

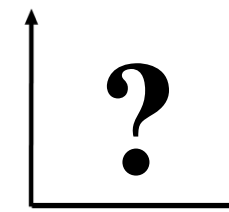


S Parameters of Trace + Bumps

De-embedding



S Parameters of Trace



S Parameters of Bumps

De-embedding Applications:

- Simulation Debugging.
- Fixture's Error Removal.
- Access to inaccessible structures.

The extreme importance of accurate parasitic de-embedding techniques to RF device characterization has already been established. In general, the parasitic contributions of device-under-test (DUT) structures mainly arise from probe pads, the interconnection lines connected to the intrinsic on chip DUT structure. **De-embedding techniques can be classified as two groups:**

□ The first group is called the **cascade based** technique **for large DUT structures:**

- TRL
- 2X Thru
- 1X Fixture

□ The second group is called the **lumped equivalent circuit model based** technique **for short DUT structures:**

- $L_i L_j$
- Hybrid Method
- L-2L

- **TRL:** While a minimum of **three measurements** (under different excitation conditions, i.e., values of a_2/a_1) are required in each of the **thru** and **line** connections, only a single measurement is required with the **reflect** connection (for line measuring, the **line** must be **lossless** or $S_{12} = S_{21}, = 0$.)

$$T_{DUT} = [T_{Error\ Box\ A}]^{-1} \times [T_{Total}] \times [T_{Error\ Box\ B}]^{-1}$$

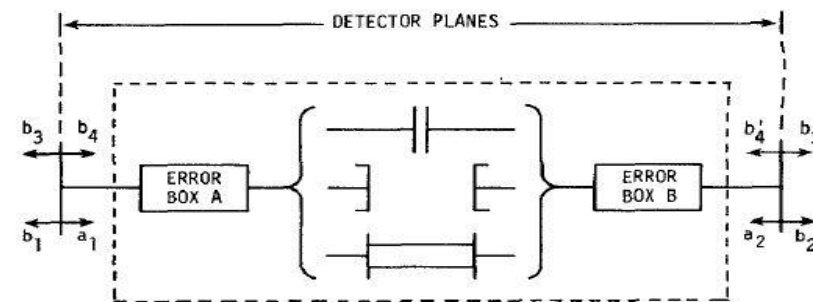
- **2X Thru:** the S11 left and right fixtures are calculated from **the time domain**, while the S21 and S22 fixtures are obtained from the wave peeling algorithm. **only 2X thru pattern is needed.**

- Symmetry in the 2x Thru is assumed.
- Minimum spacing between discontinuities in the 2x Thru is needed.

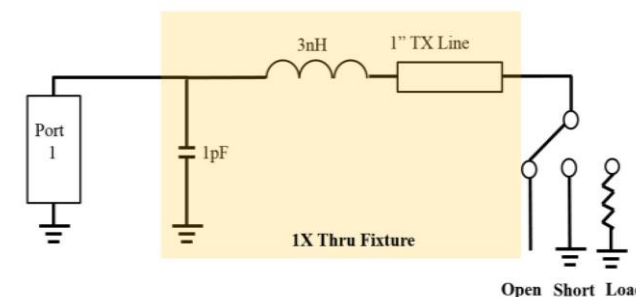
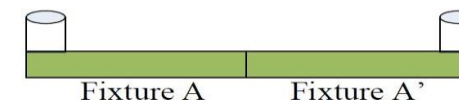
$$T_{DUT} = [T_{Fixture_A}]^{-1} \times [T_{Total}] \times [T_{Fixture_A'}]^{-1}$$

- **1X Fixture:** This proposed de-embedding method only **requires two calibration patterns** to obtain the DUT S-parameter, as depicted in the Figure. In this design, **1X left and 1X right are not necessarily symmetric**, and are **characterized separately.**

$$T_{DUT} = [T_{Fixture_A}]^{-1} \times [T_{Total}] \times [T_{Fixture_B}]^{-1}$$



Ref: Thru-Reflect-Line: An Improved Technique for Calibrating the Dual Six-Port Automatic Network Analyzer, 1979



Ref: 2X-Thru, 1X-Reflection, and Thru-Line de-embedding: Theory, sensitivity analysis, and error corrections, 2019

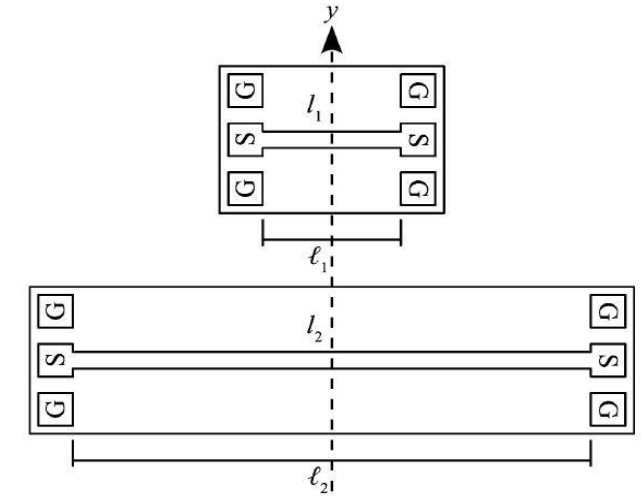
➤ **$L_i L_j$:** The $L_i L_j$ de-embedding method also **requires the measurement of two transmission lines**. These transmission lines, however, may be any two different lengths; one transmission line does not have to be double the length of the other. Further, **probing pads are only modeled** as a shunt admittance, **$Y=j\omega C$** . Individual pads are still assumed to be symmetric. Using **ABCD parameters**, a transmission line of length i can be represented as the following cascade of ABCD matrices:

$$ABCD_{meas_Li\&Lj}=ABCD_{LP}ABCD_{Li\&Lj}ABCD_{RP}$$

$$ABCD_{hybrid}=ABCD_{meas_Lj}ABCD_{meas_Li}^{-1}=ABCD_{LP}ABCD_{Lj-Li}ABCD_{LP}^{-1}$$

$$Y_{hybrid}=Y_{Lj-Li}+\begin{bmatrix} Y & 0 \\ 0 & -Y \end{bmatrix}=\begin{bmatrix} Y_{11} & Y_{12} \\ Y_{21} & Y_{22} \end{bmatrix}$$

$$Y_{Lj-Li}=\frac{Y_{hybrid}+Swap(Y_{hybrid})}{2}$$



Ref: De-embedding transmission line measurements for accurate modeling of IC designs, (in IEEE Transactions on Electron Devices, 2006)

➤ **Hybrid Method:** For the proposed hybrid de-embedding method, the measurement of three transmission lines is required. One line is of **length L** , another is of **length $2L$** , and the final line is a short line of **length L_i** . Similar to the L - $2L$ de-embedding technique, probing pads are modeled with both a shunt admittance and a series impedance. However, the proposed hybrid method switches the order of these lumped parasitic so that the **series impedance is first**. The **shunt admittance then follows the series impedance**, as shown in the Fig.

$$ABCD_{thru}=ABCD_{meas_}ABCD_{meas_2L}^{-1}ABCD_{meas_L}$$

$$=ABCD_{LP}ABCD_{RP}$$

$$ABCD_{2L\ no\ Z}=ABCD_Z^{-1}ABCD_{meas_2L}ABCD_Z^{-1}$$

$$ABCD_{L\ no\ Z}=ABCD_Z^{-1}ABCD_{meas_L}ABCD_Z^{-1}$$

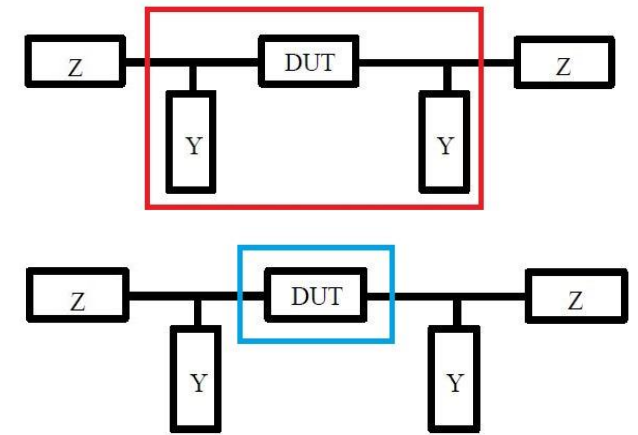
$$ABCD_{Li\ no\ Z}=ABCD_Z^{-1}ABCD_{meas_Li}ABCD_Z^{-1}$$

$$ABCD_{2L-Li\ (Hybrid)}=ABCD_{2L\ no\ Z}ABCD_{Li\ no\ Z}^{-1}$$

$$ABCD_{L-Li\ (Hybrid)}=ABCD_{L\ no\ Z}ABCD_{Li\ no\ Z}^{-1}$$

$$Y_{2L-Li}=\frac{Y_{2L-Li\ (Hybrid)}+Swap(Y_{2L-Li\ (Hybrid)})}{2}$$

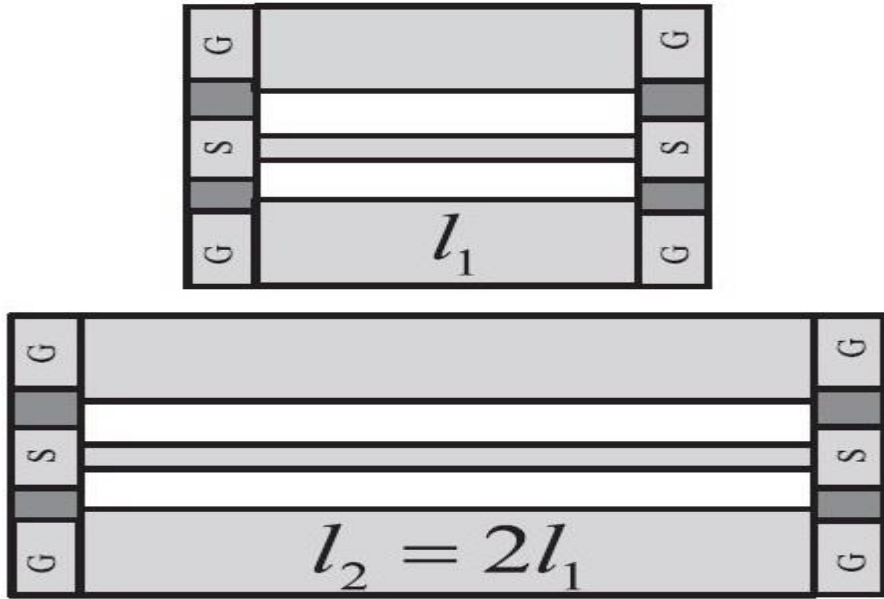
$$Y_{L-Li}=\frac{Y_{L-Li\ (Hybrid)}+Swap(Y_{L-Li\ (Hybrid)})}{2}$$



Ref: De-embedding techniques for transmission lines: An exploration, review, and proposal, 2013

L-2L Method (1)

8



Ref: Evaluation of a Multi-Line De-embedding Technique up to 110GHz for Millimeter-Wave CMOS Circuit Design

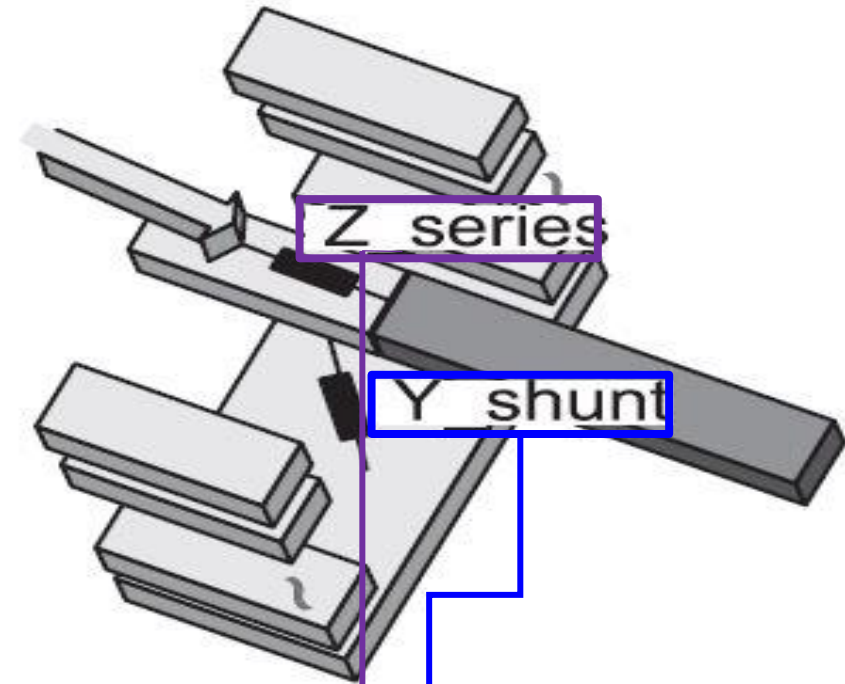
$$ABCD_{meas_L} = ABCD_{LP} ABCD_L ABCD_{RP}$$

$$ABCD_{LP} = ABCD_Y ABCD_Z$$

$$ABCD_{RP} = ABCD_Z ABCD_Y$$

Where,
 $ABCD_{LP}$ represents the matrix of the left pad;
 $ABCD_L$ represents the matrix of the txline of length L ;
 $ABCD_{RP}$ represents the matrix of the right pad.

Where,
 $ABCD_Y$ represents the shunt admittance;
 $ABCD_Z$ represents the series impedance.



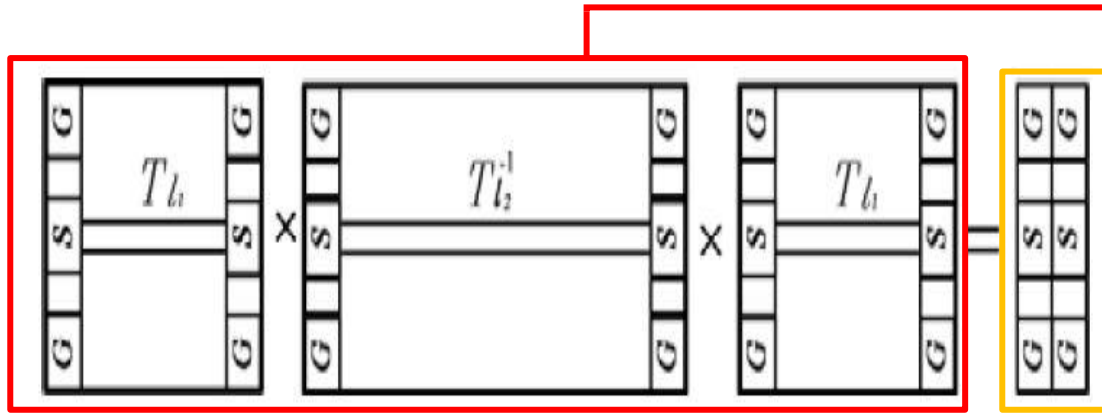
$$ABCD_Y = \begin{bmatrix} 1 & 0 \\ Y & 1 \end{bmatrix} \rightarrow Y = j\omega C$$

$$ABCD_Z = \begin{bmatrix} 1 & Z \\ 0 & 1 \end{bmatrix} \rightarrow Z = R + j\omega L$$

Ref: De-embedding techniques for transmission lines: An exploration, review, and proposal, 2013

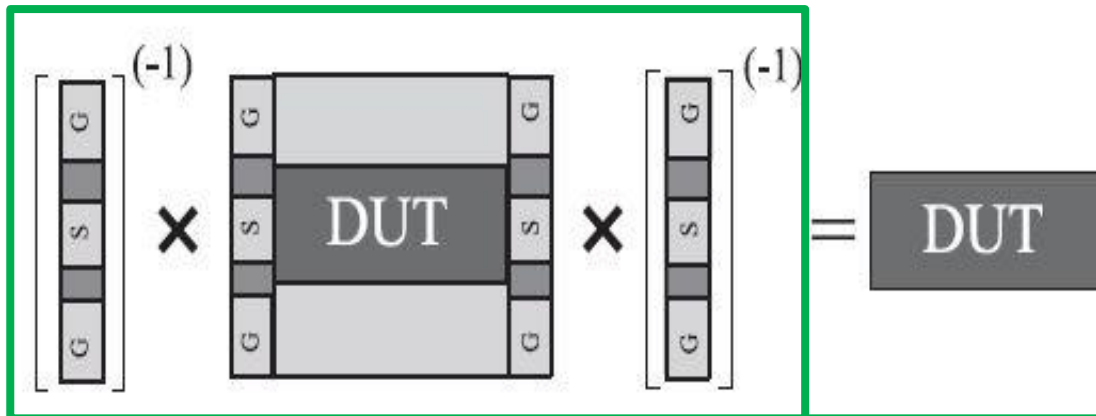
L-2L Method (2)

9



$$\begin{aligned}
 ABCD_{thru} &= ABCD_{meas_L} ABCD_{meas_2L}^{-1} ABCD_{meas_L} \\
 &= \underline{ABCD_{LP} ABCD_{RP}} \\
 &= \begin{pmatrix} 2Y_{shunt}Z_{series} + 1 & 2Z_{series} \\ 2Y_{shunt}(Y_{shunt}Z_{series} + 1) & 2Y_{shunt}Z_{series} + 1 \end{pmatrix}
 \end{aligned}$$

Ref: Evaluation of a Multi-line De-embedding Technique for Millimeter-Wave CMOS Circuit Design_ Proceeding of Asia-Pacific Microwave Conference



Ref: Evaluation of a Multi-Line De-embedding Technique up to 110GHz for Millimeter-Wave

$$\begin{aligned}
 ABCD_{LP} &= ABCD_Y ABCD_Z \\
 ABCD_{RP} &= ABCD_Z ABCD_Y
 \end{aligned}$$

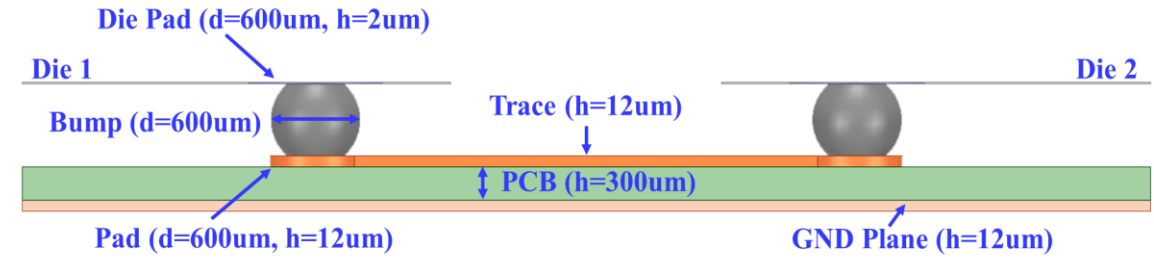
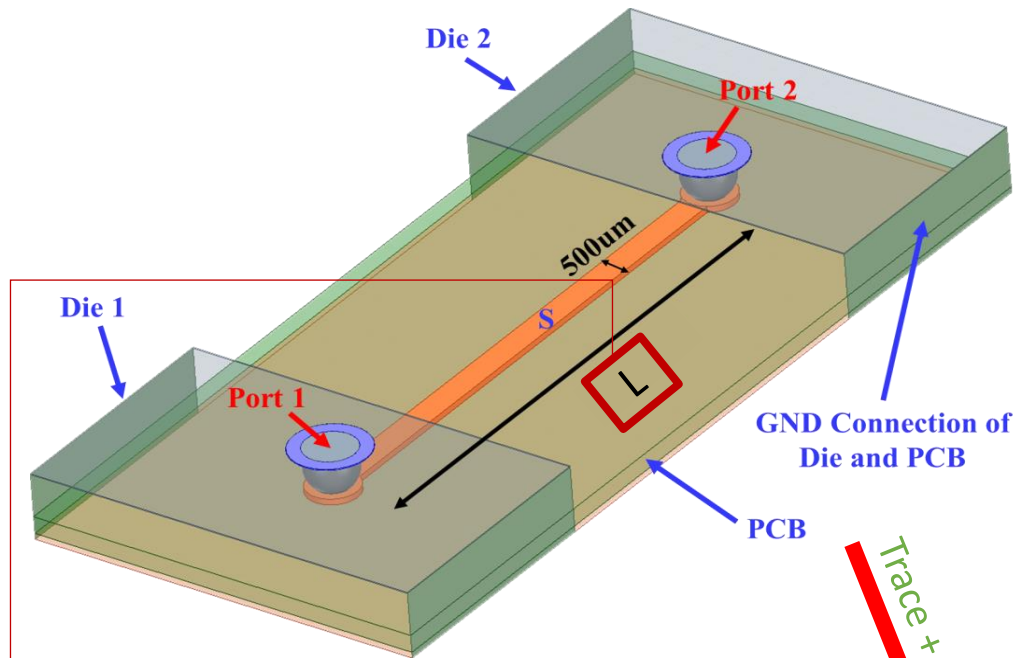
$$\begin{aligned}
 ABCD_Y &= \begin{bmatrix} 1 & 0 \\ Y & 1 \end{bmatrix} \\
 ABCD_Z &= \begin{bmatrix} 1 & Z \\ 0 & 1 \end{bmatrix}
 \end{aligned}$$

$$ABCD_{meas_L} = ABCD_{LP} ABCD_L ABCD_{RP}$$

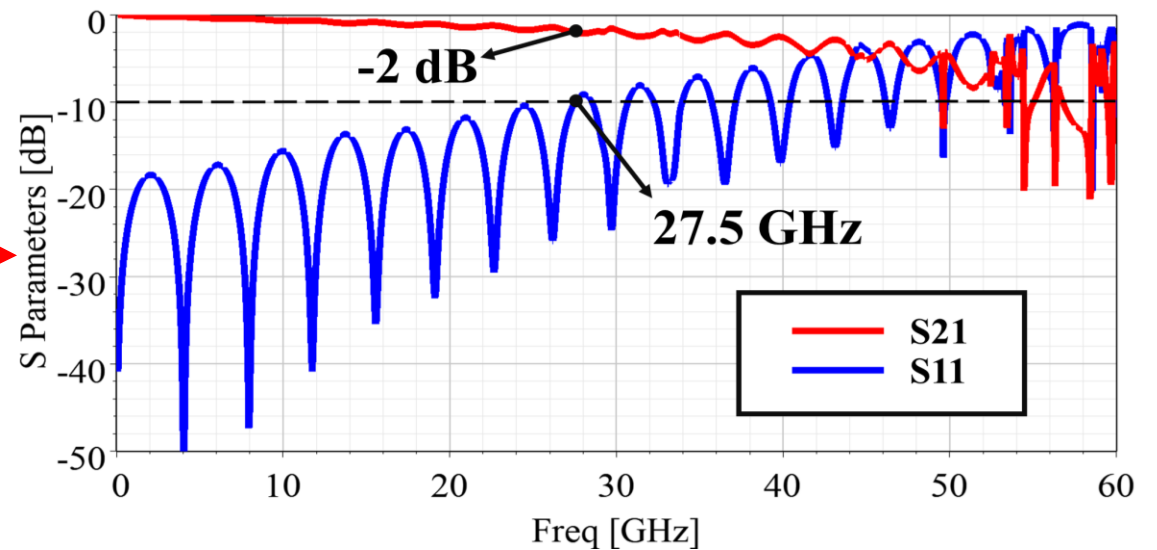
$$ABCD_L = \underline{ABCD_{LP}^{-1} ABCD_{meas_L} ABCD_{RP}^{-1}}$$

Trace + Bump Structure and Simulation

10



$$S_{11}=S_{22} , S_{21}=S_{12}$$



L-2L
Method

L: 12.7mm
2L: 25.4mm

L: 1.5mm
2L: 3mm

1

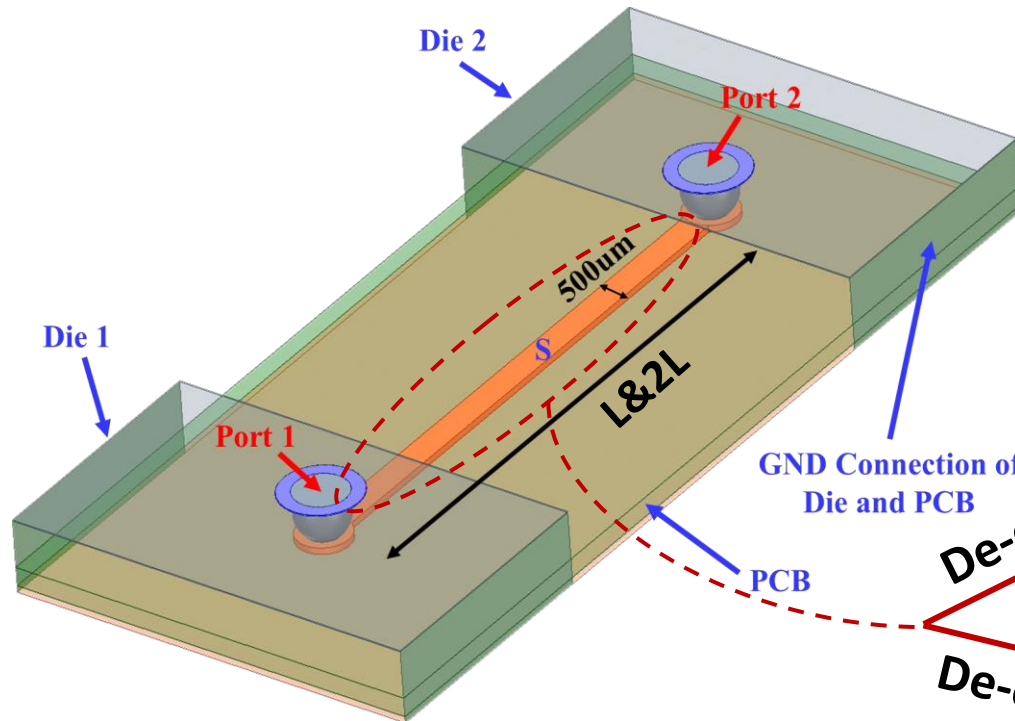
2

S-Parameters

Trace + Bump

1: S-Parameter Extraction Traces By L-2L Method

11



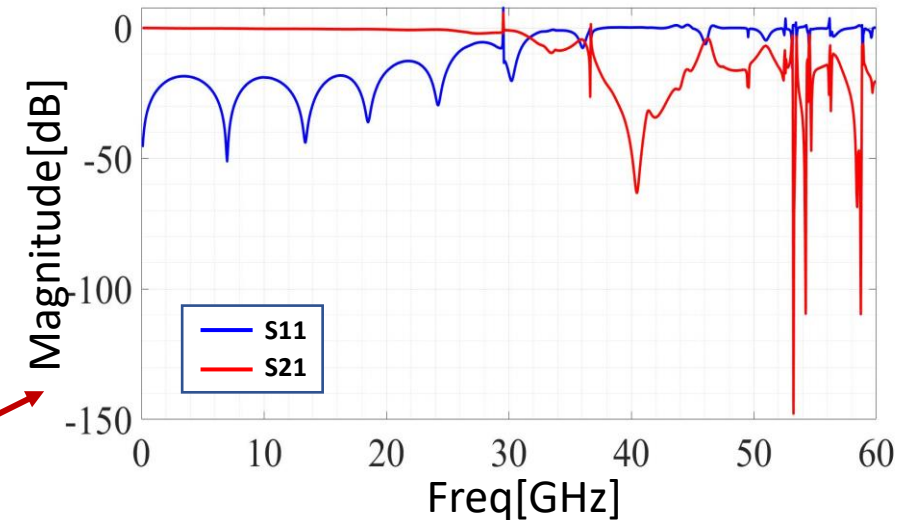
S-Parameter extracted of trace from **L-2L Method:**

- $L = 12.7\text{mm}$ (half inch)
- $2L = 25.4\text{mm}$ (an inch)

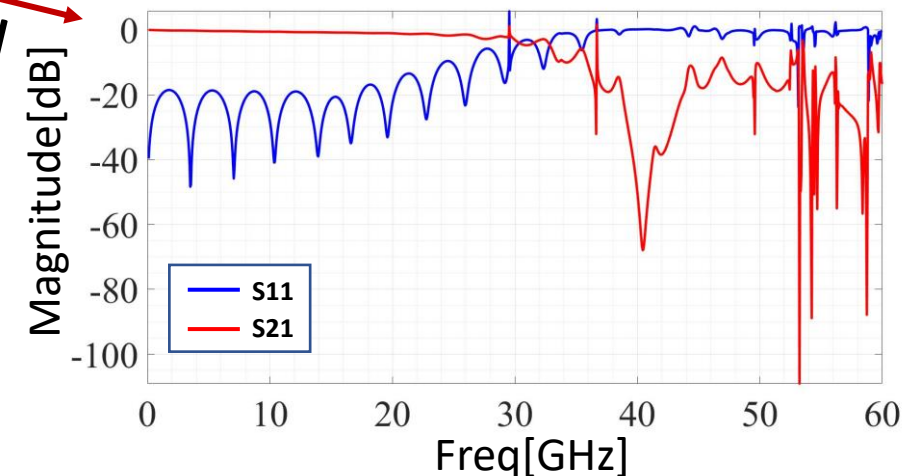
Ref: Technical report, 2020 by Pouya Namaki and Nasser Masoumi

De-embedded

De-embedded



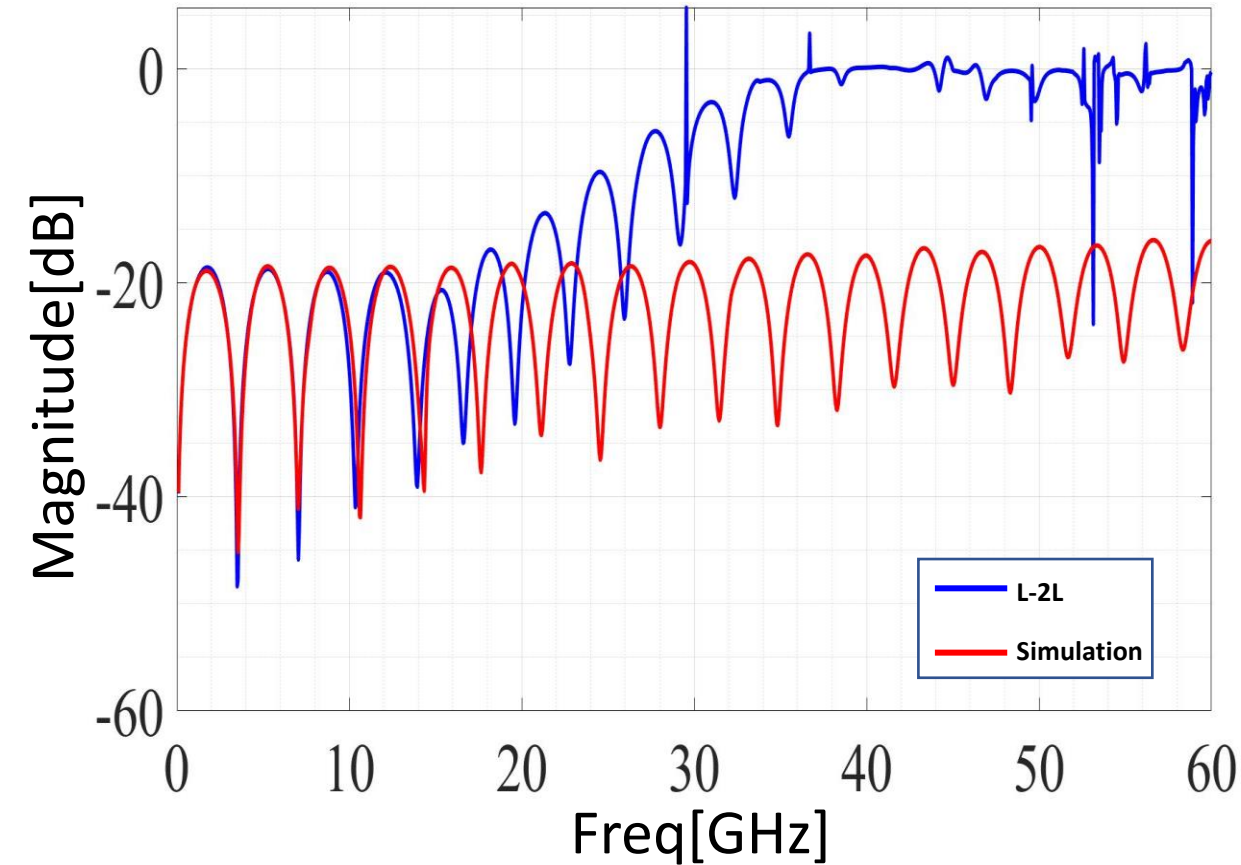
S11 and S21 of the line with a Length of L (12.7mm or half Inch)



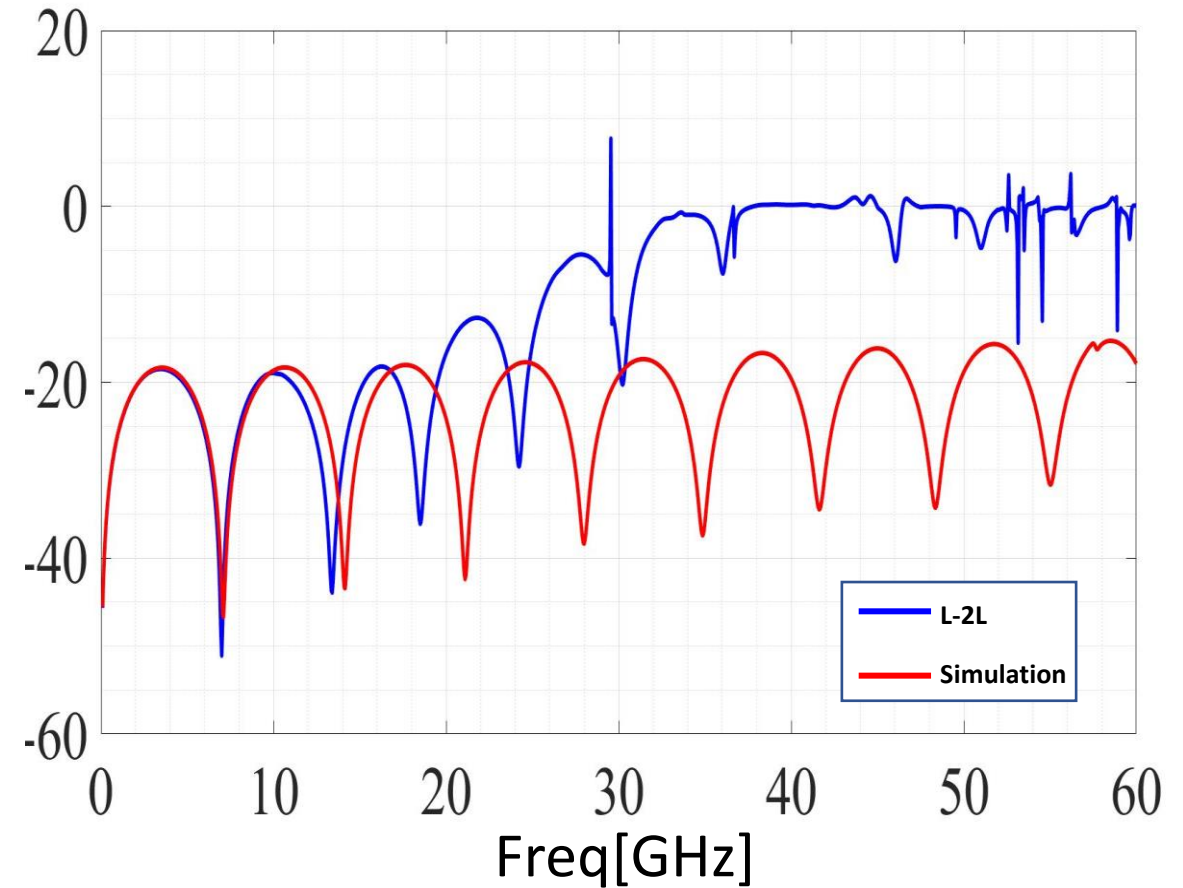
S11 and S21 of the line with a Length of 2L (25.4mm or an Inch)

S-Parameter Extraction Traces By L-2L Compare to Simulation

12



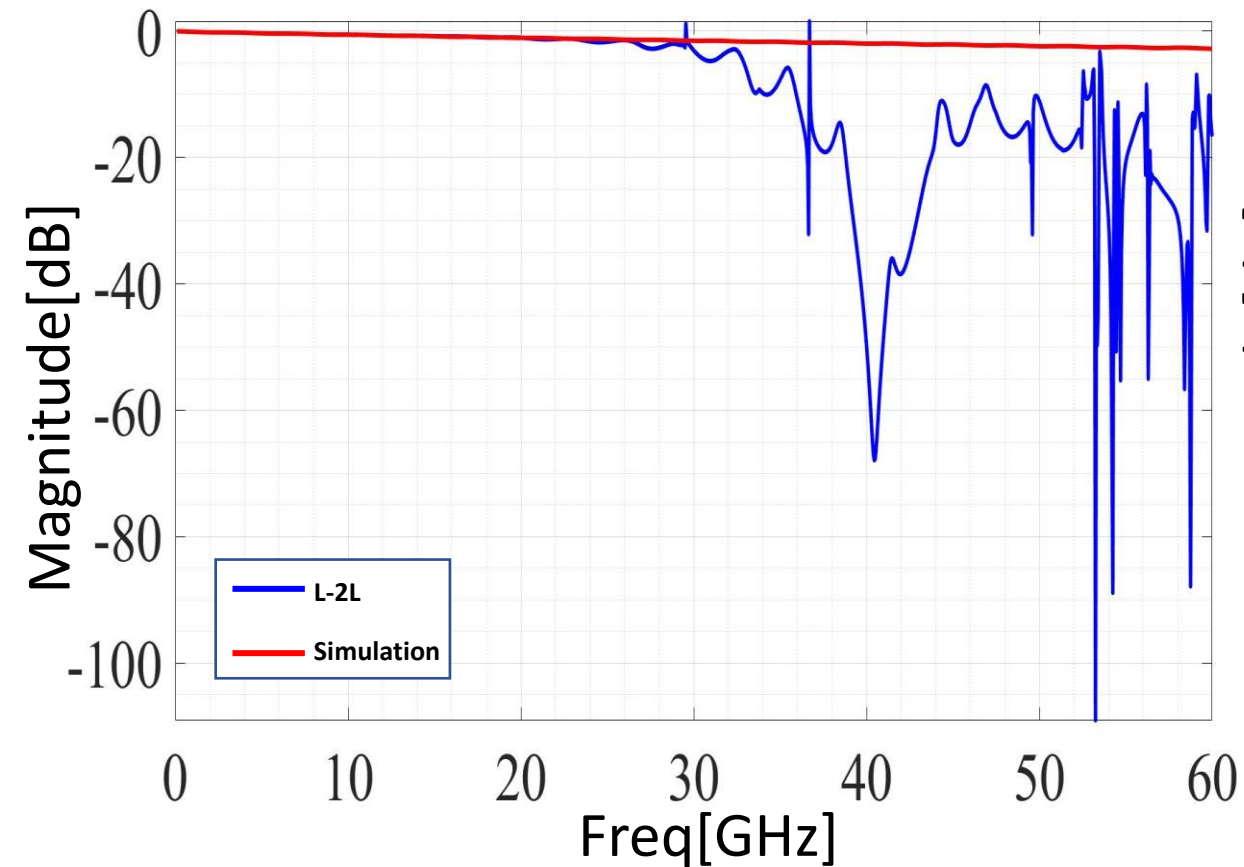
S11 of line with length of **2L** from **L-2L method** and **simulation**



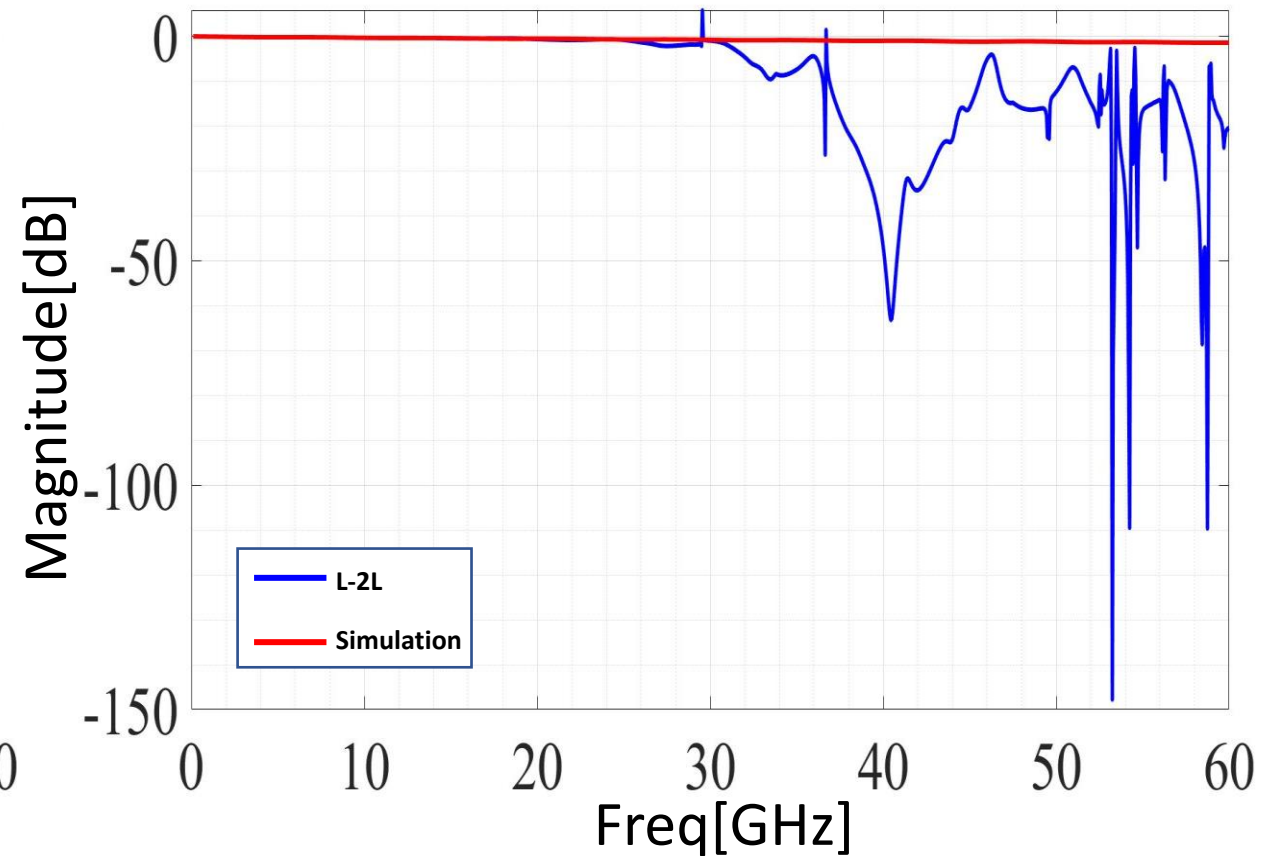
S11 of line with length of **L** from **L-2L method** and **simulation**

S-Parameter Extraction Traces By L-2L Compare to Simulation (2)

13



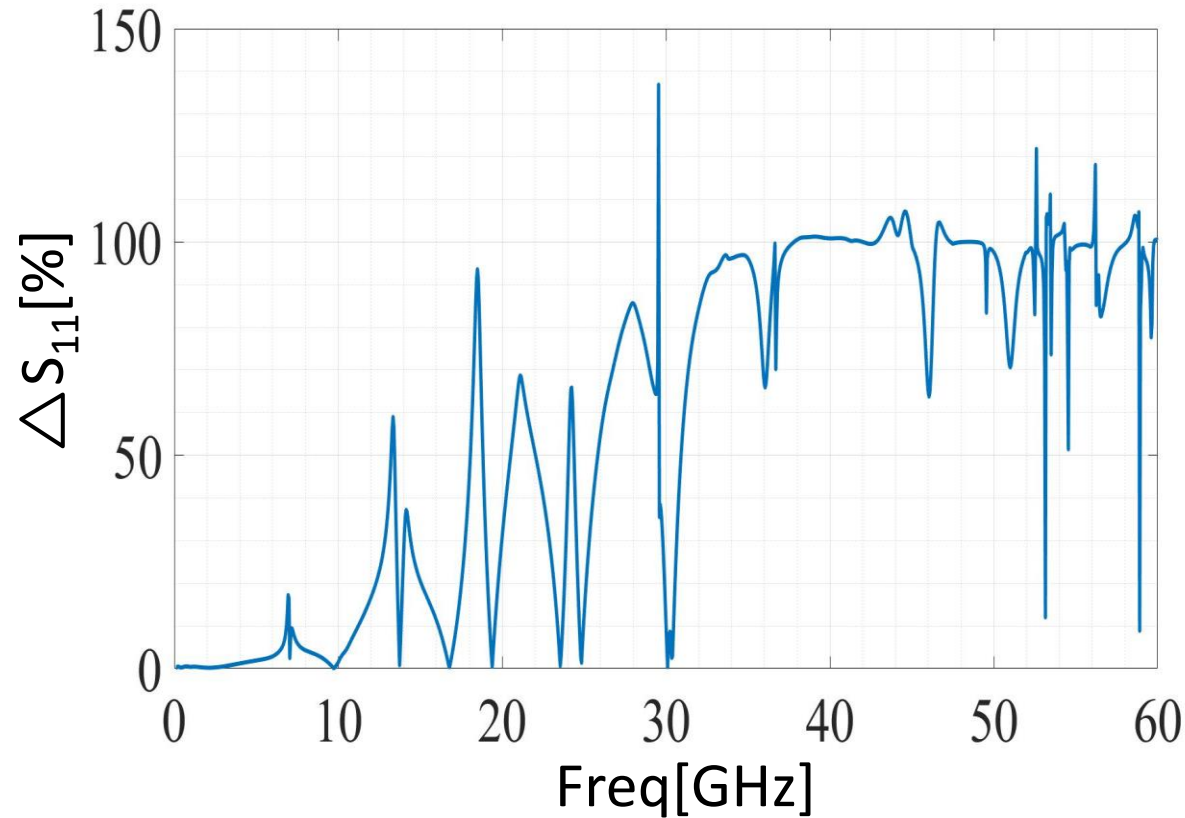
S21 of line with length of **2L** from **L-2L method** and **simulation**



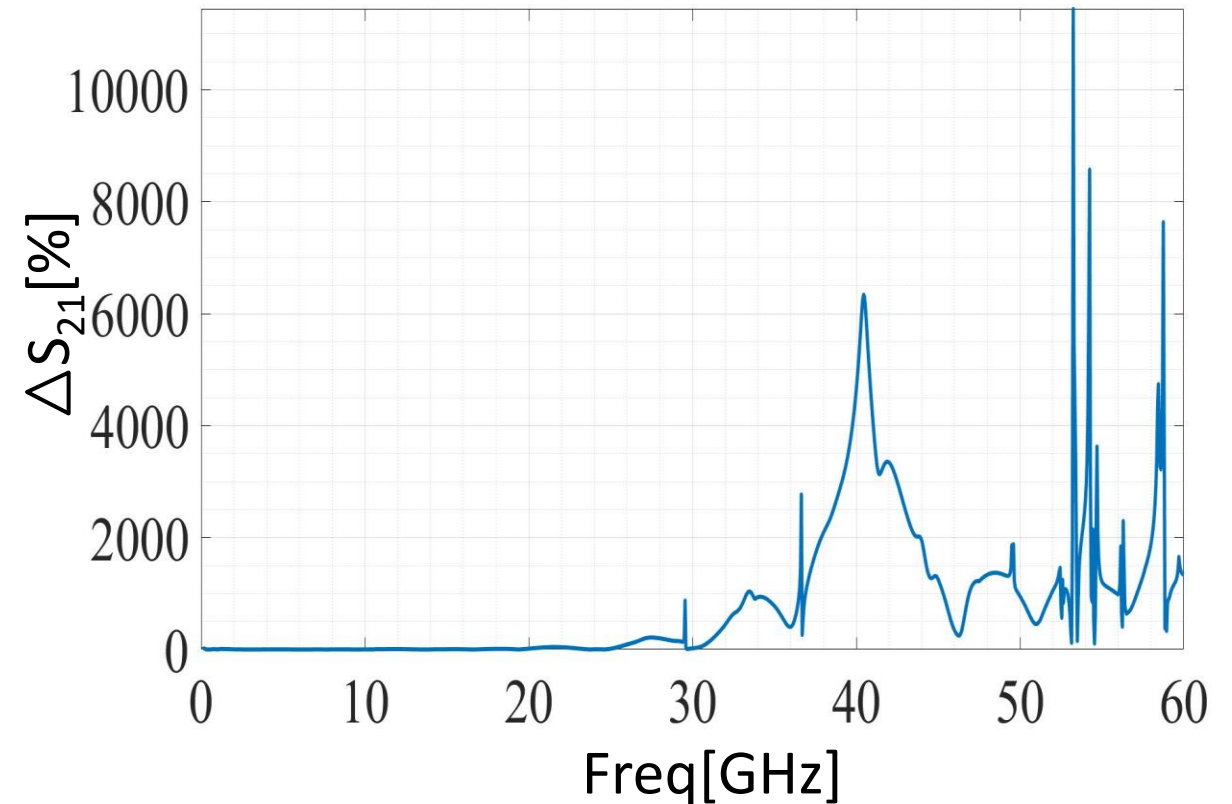
S21 of line with length of **L** from **L-2L method** and **simulation**

Error of L S-Parameter Due Frequency

14



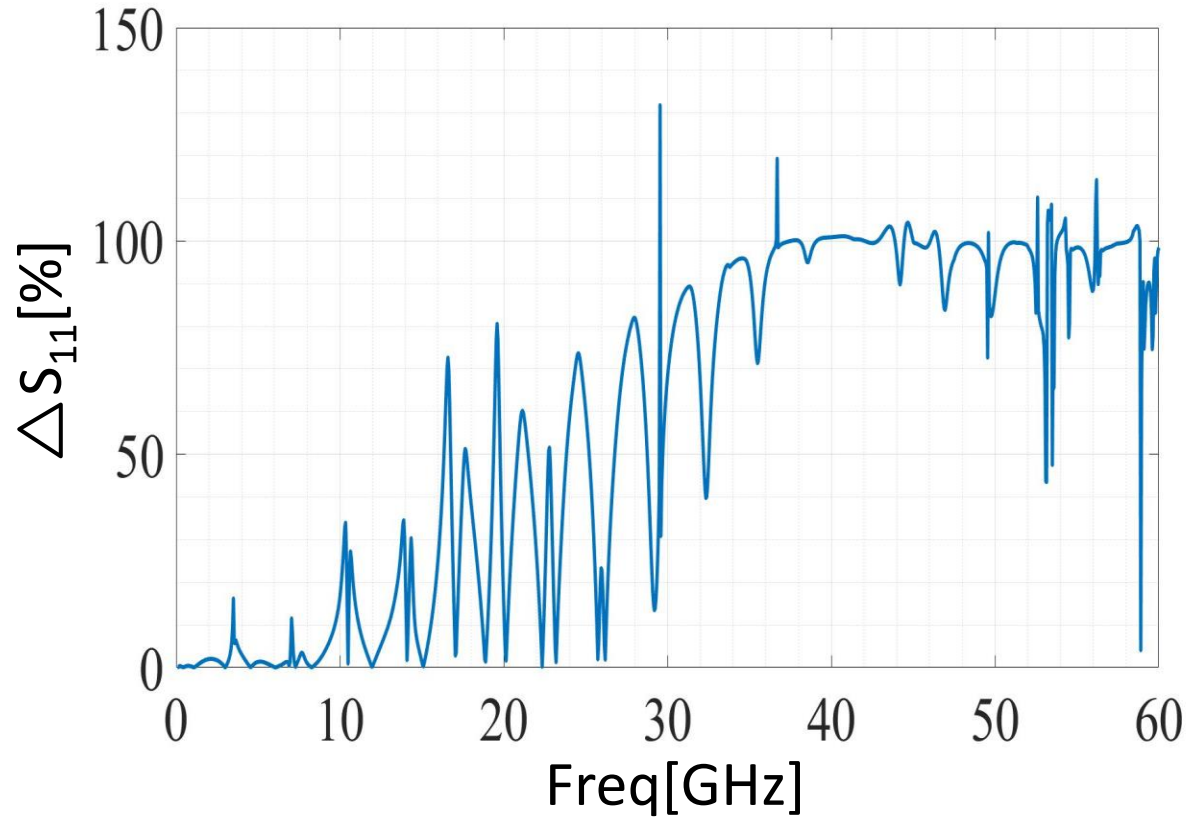
S_{11} error of L (12.7mm) line



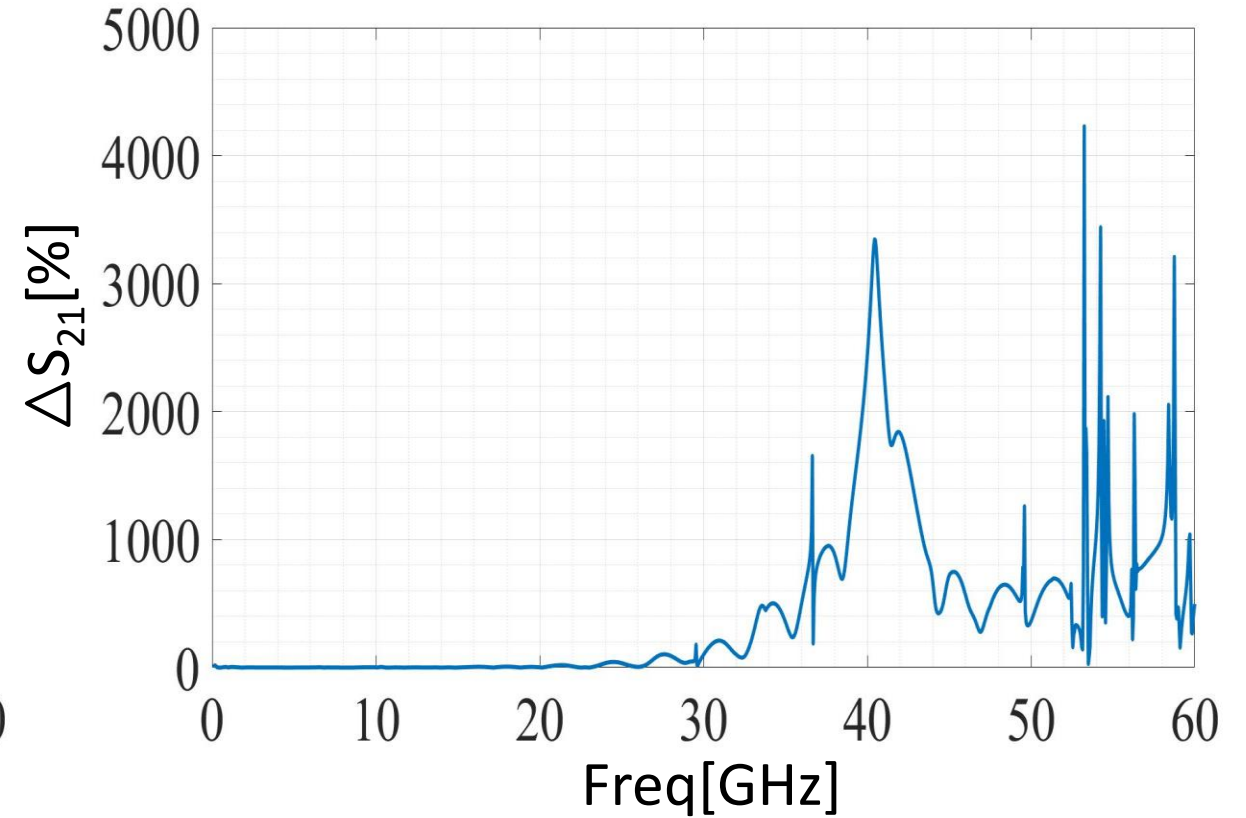
S_{21} error of L (12.7mm) line

Error of 2L S-Parameter Due Frequency

15



S_{11} error of 2L (25.4mm) line



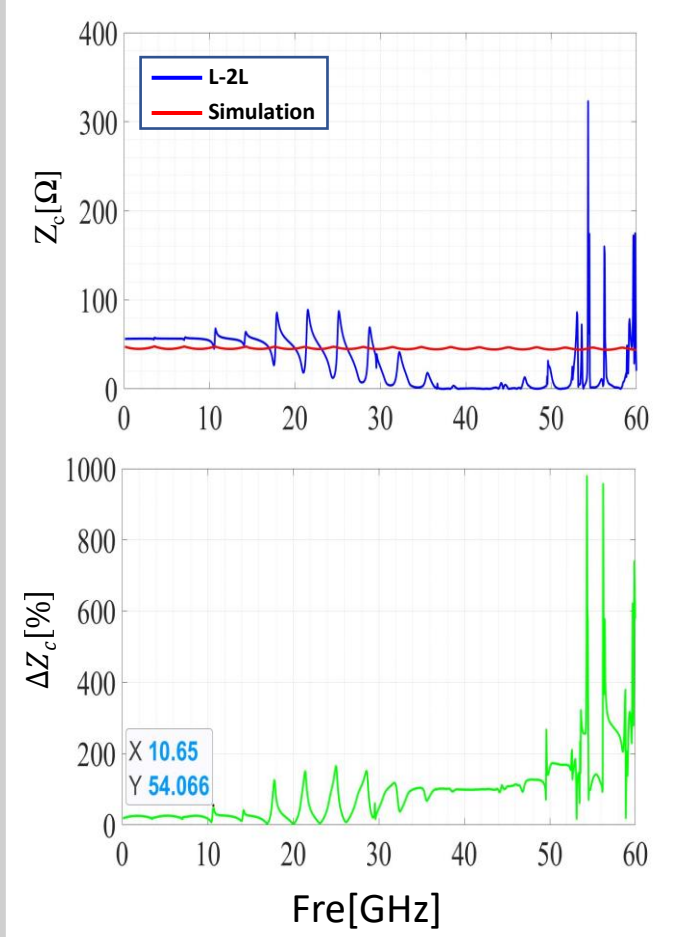
S_{21} error of 2L (25.4mm) line

Characteristics Line's Impedance

16

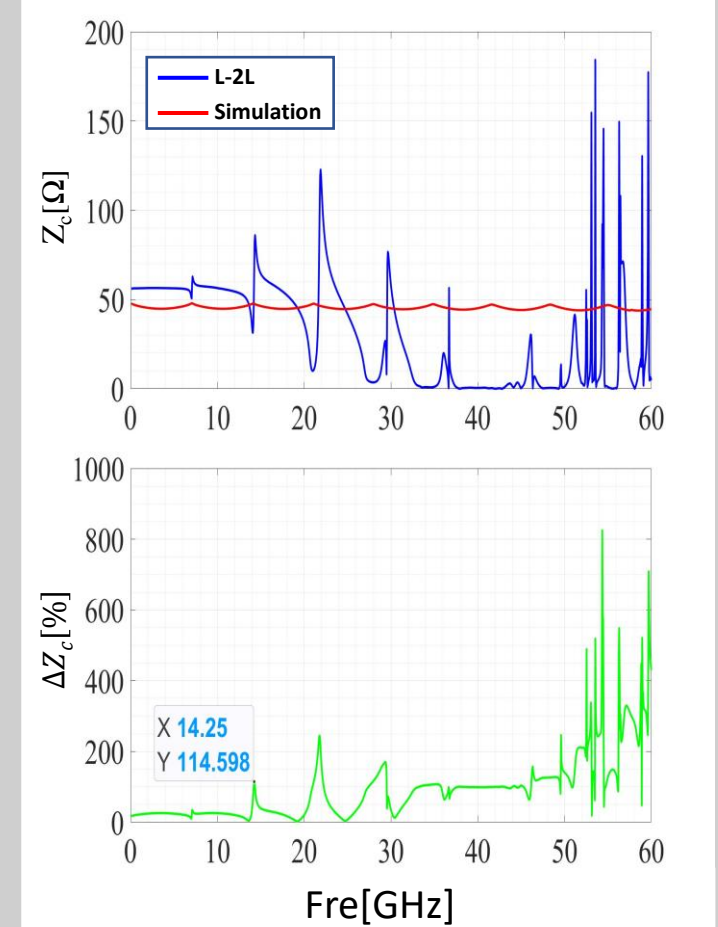
The computation's error of characteristics impedance causes in **10.65GHz (2L)**

$$Z = Z_0 \left\{ \frac{(1 + S_{11})^2 - S_{21}^2}{(1 - S_{11})^2 - S_{21}^2} \right\}^{\frac{1}{2}}$$



The computation's error of characteristics impedance causes in **14.25GHz (L)**

$$Z = Z_0 \left\{ \frac{(1 + S_{11})^2 - S_{21}^2}{(1 - S_{11})^2 - S_{21}^2} \right\}^{\frac{1}{2}}$$



- By using the measured S-Parameter the parasites of the pad can be calculated which is modeled as a **π -type** lumped constant circuit. However, in through-only method, **the length of the through-line is required to be very short** to match with the π -type lumped model.

$$\Delta = \left| \frac{X^{L-2L} - X^L}{X^L} \right|$$

- In lumped group method, an extra grounded metal strip, which adds **resistance and inductance to the short structure**, is used as a connection between the two ports.

- The parasitic contribution of the extra grounded metal strip **cannot be ignored if the frequencies are high or if the DUT structures are large.**

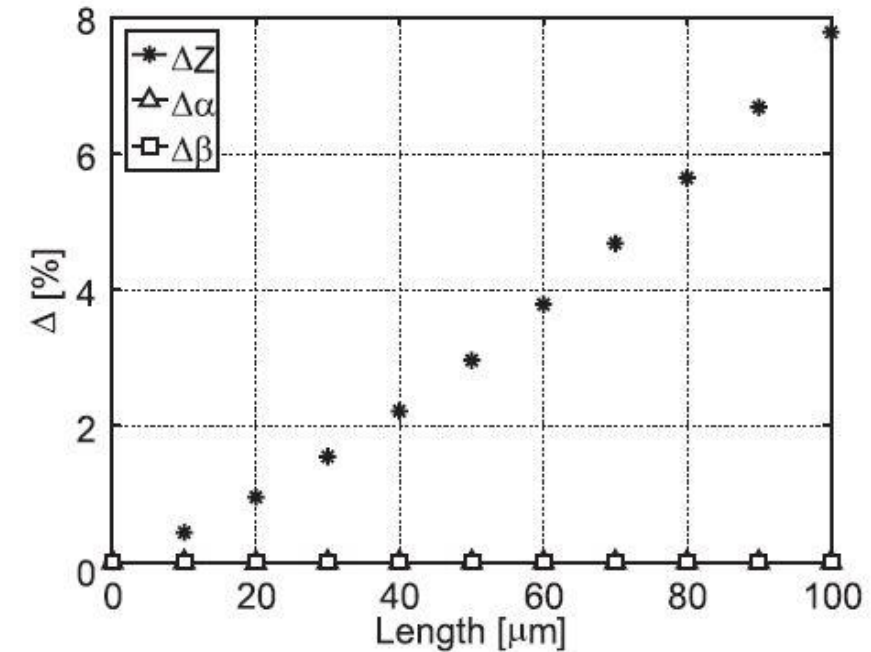
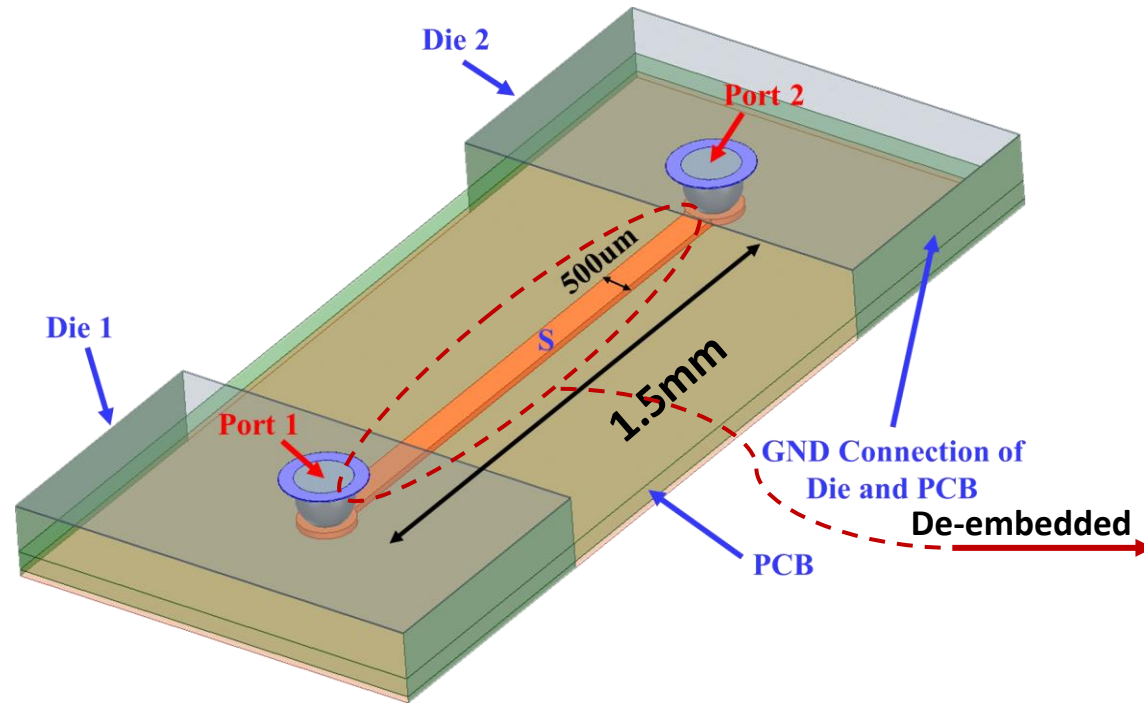


Fig. 4 Calculated results by using through-only method.

2: S-Parameter Extraction Traces By L-2L Method

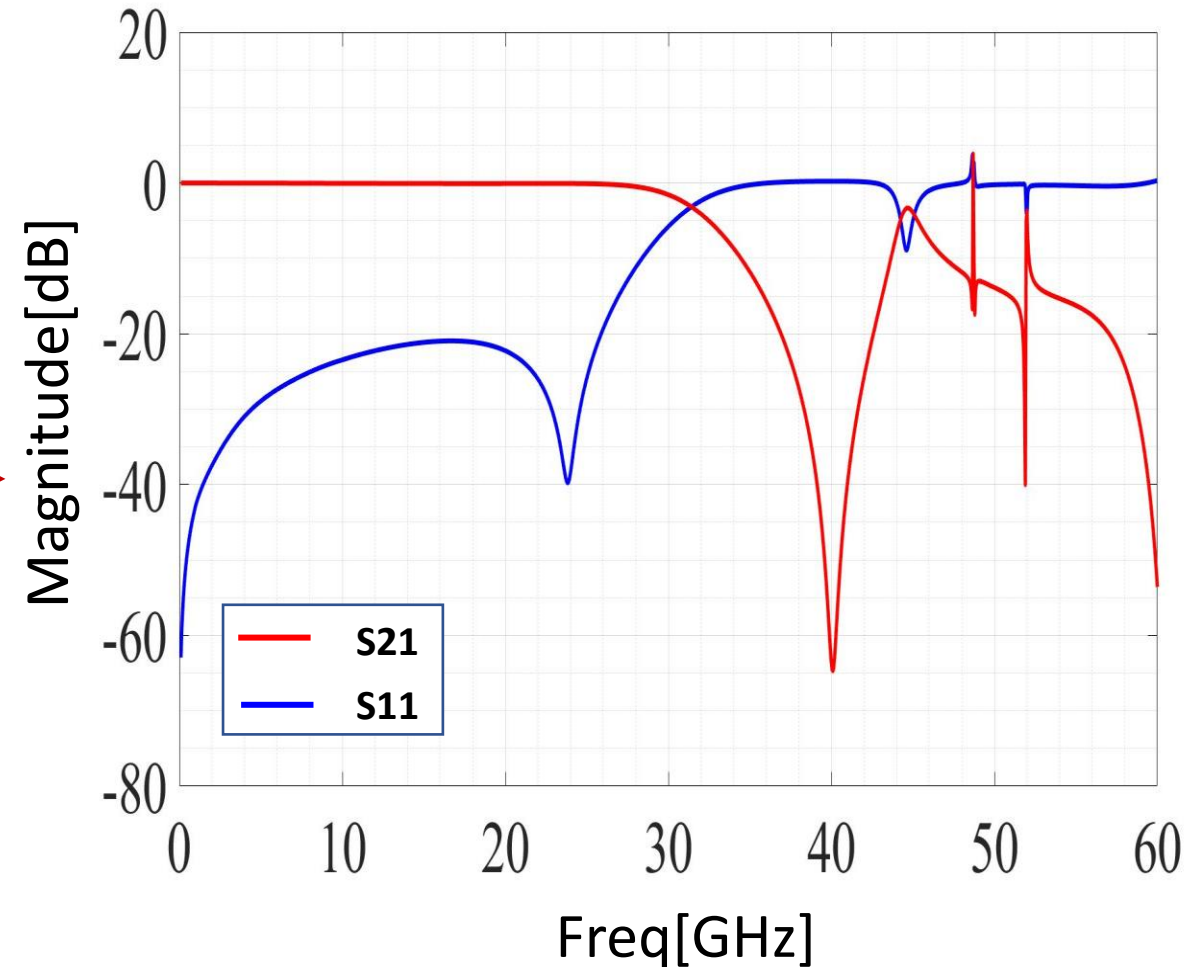
18



S-Parameter extracted of trace from **L-2L Method:**

- $L = 1.5\text{mm}$
- $2L = 3\text{mm}$

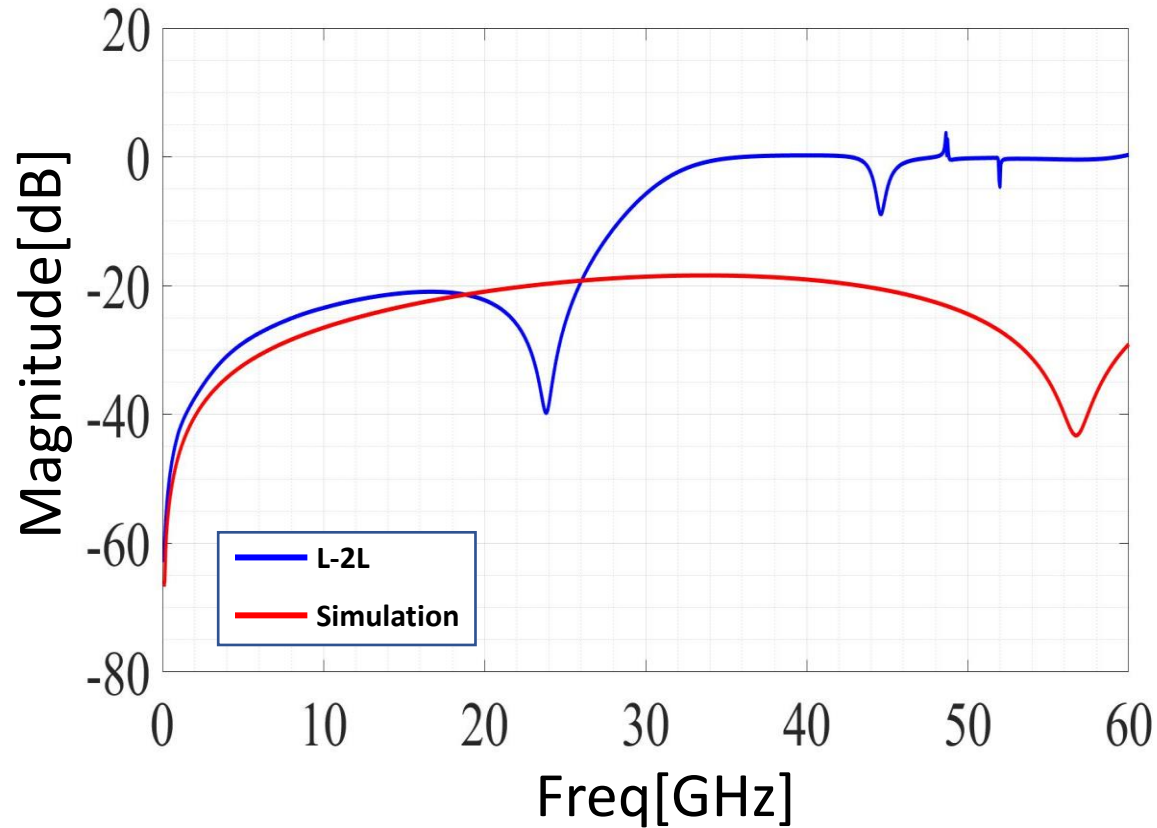
Ref: Technical report, 2020 by Pouya Namaki and Nasser Masoumi



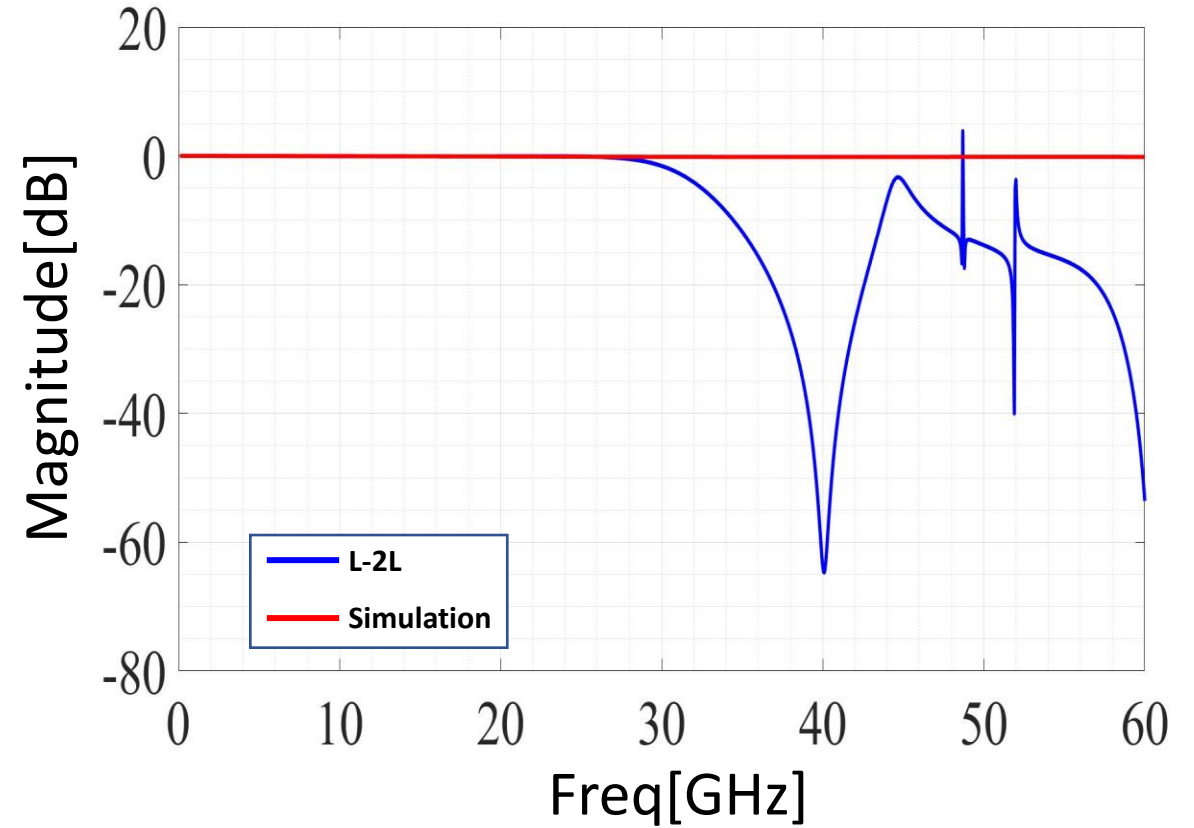
S_{11} and S_{21} of the line with a Length of L (1.5mm)

S-Parameter Extraction Traces By L-2L Compare to Simulation

19



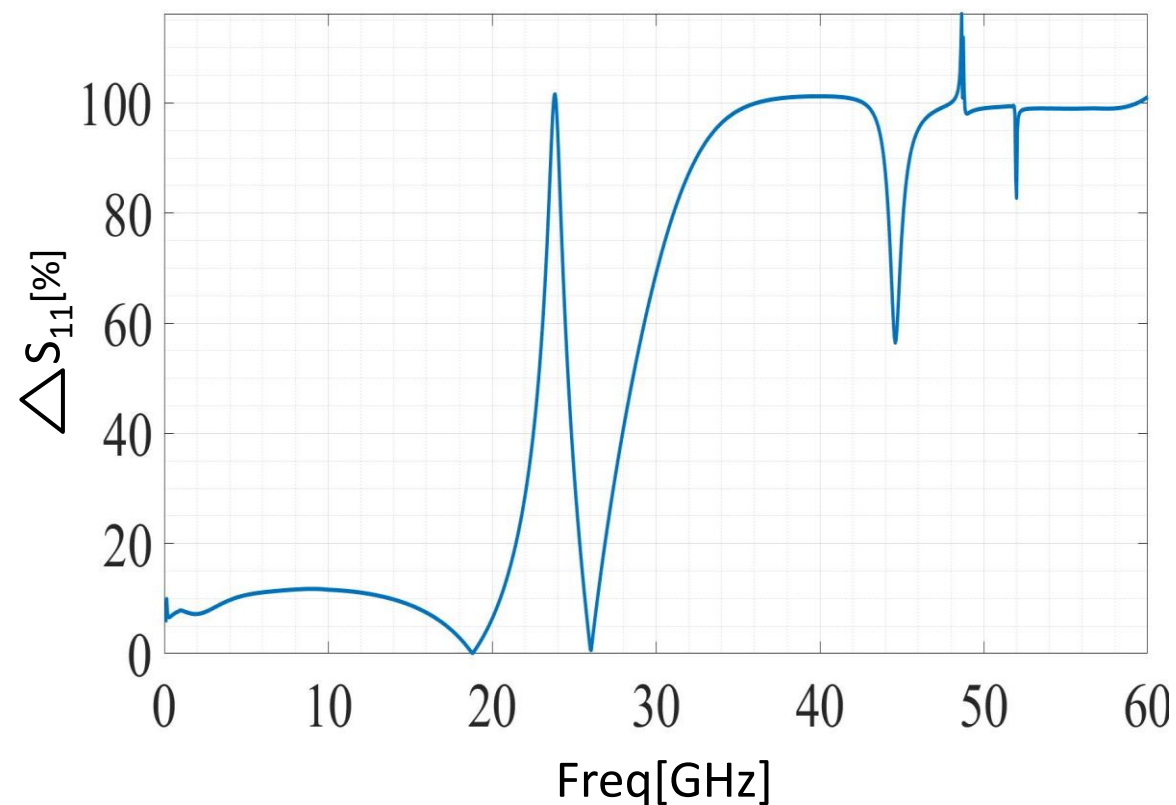
S_{11} of line with length of L from **L-2L method** and **simulation**



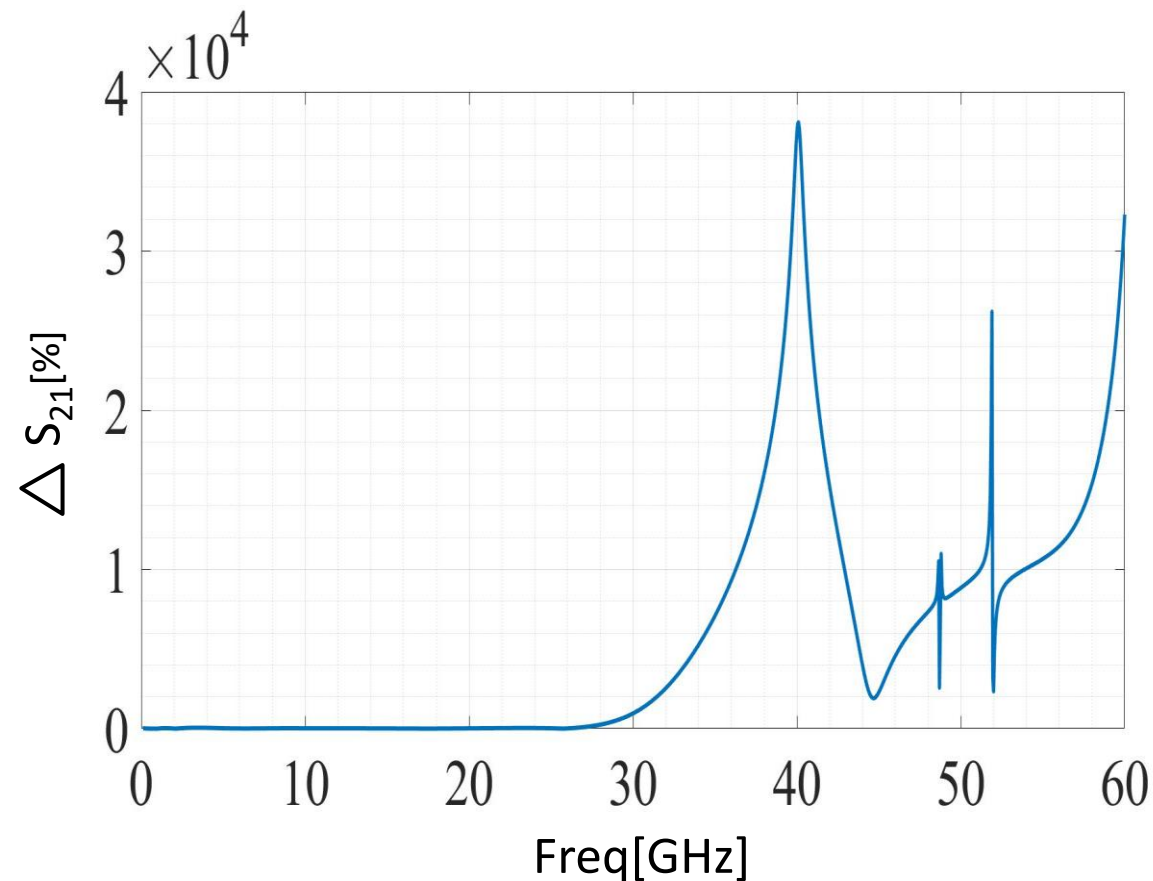
S_{21} of line with length of L from **L-2L method** and **simulation**

Error of Line's S-Parameter

20



S_{11} 's error of L (1.5mm) line



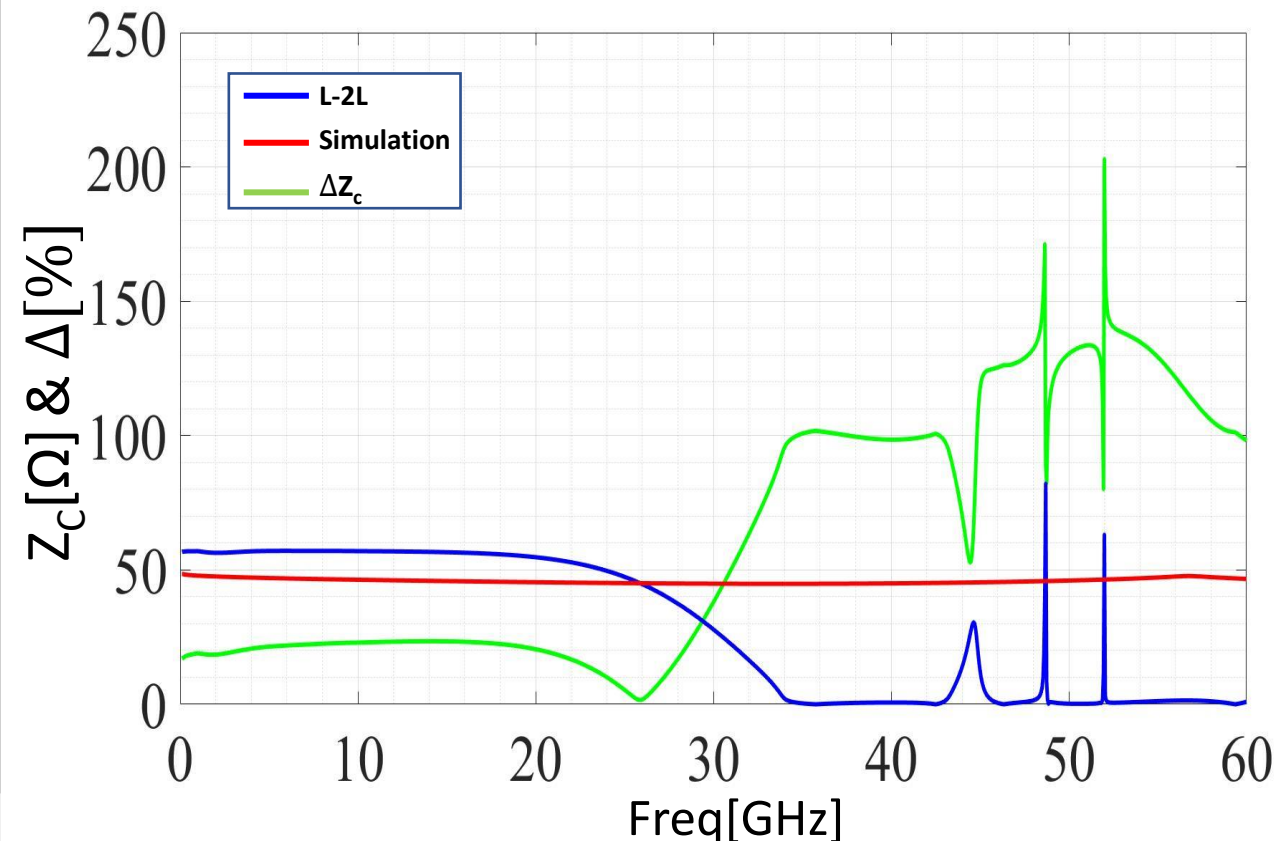
S_{21} 's error of L (1.5mm) line

The computation's error of characteristics impedance causes in 18.8GHz (L)

$$Z = Z_0 \left\{ \frac{(1 + S_{11})^2 - S_{21}^2}{(1 - S_{11})^2 - S_{21}^2} \right\}^{\frac{1}{2}}$$

L-2L Method Accuracy:

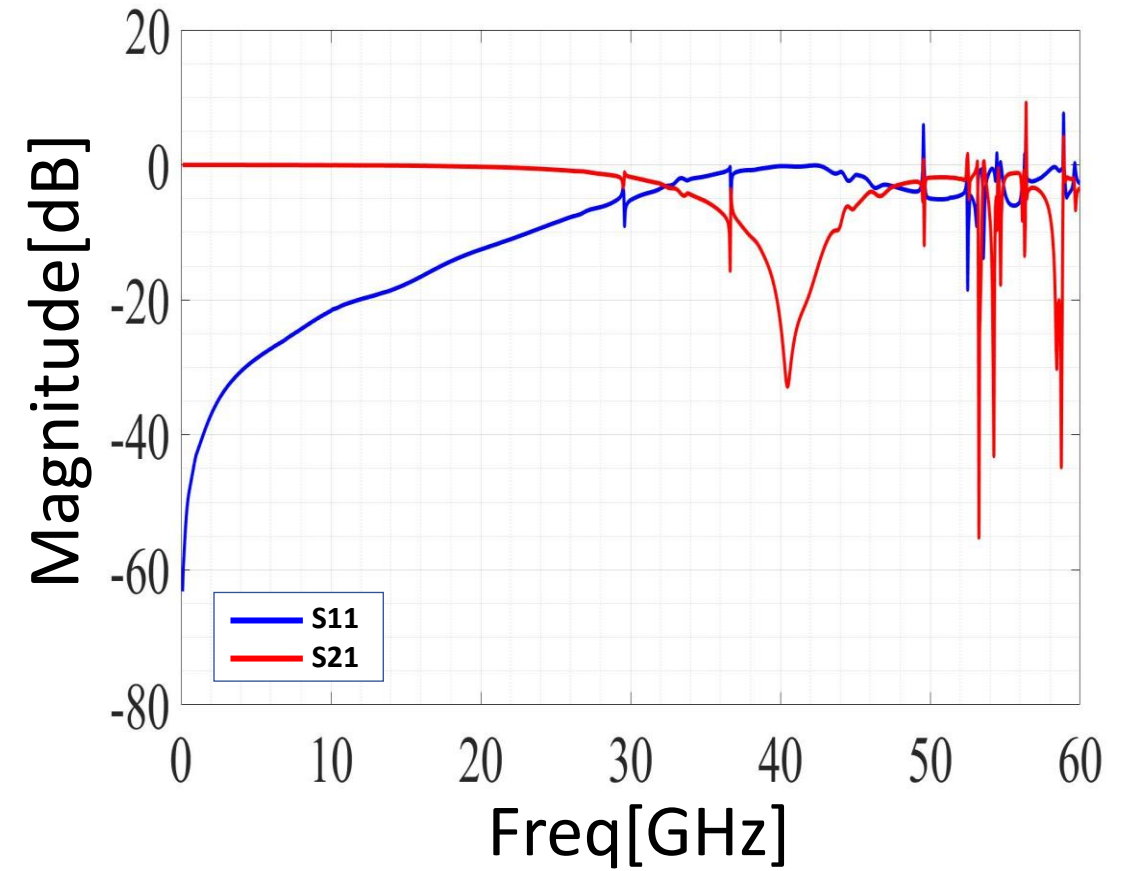
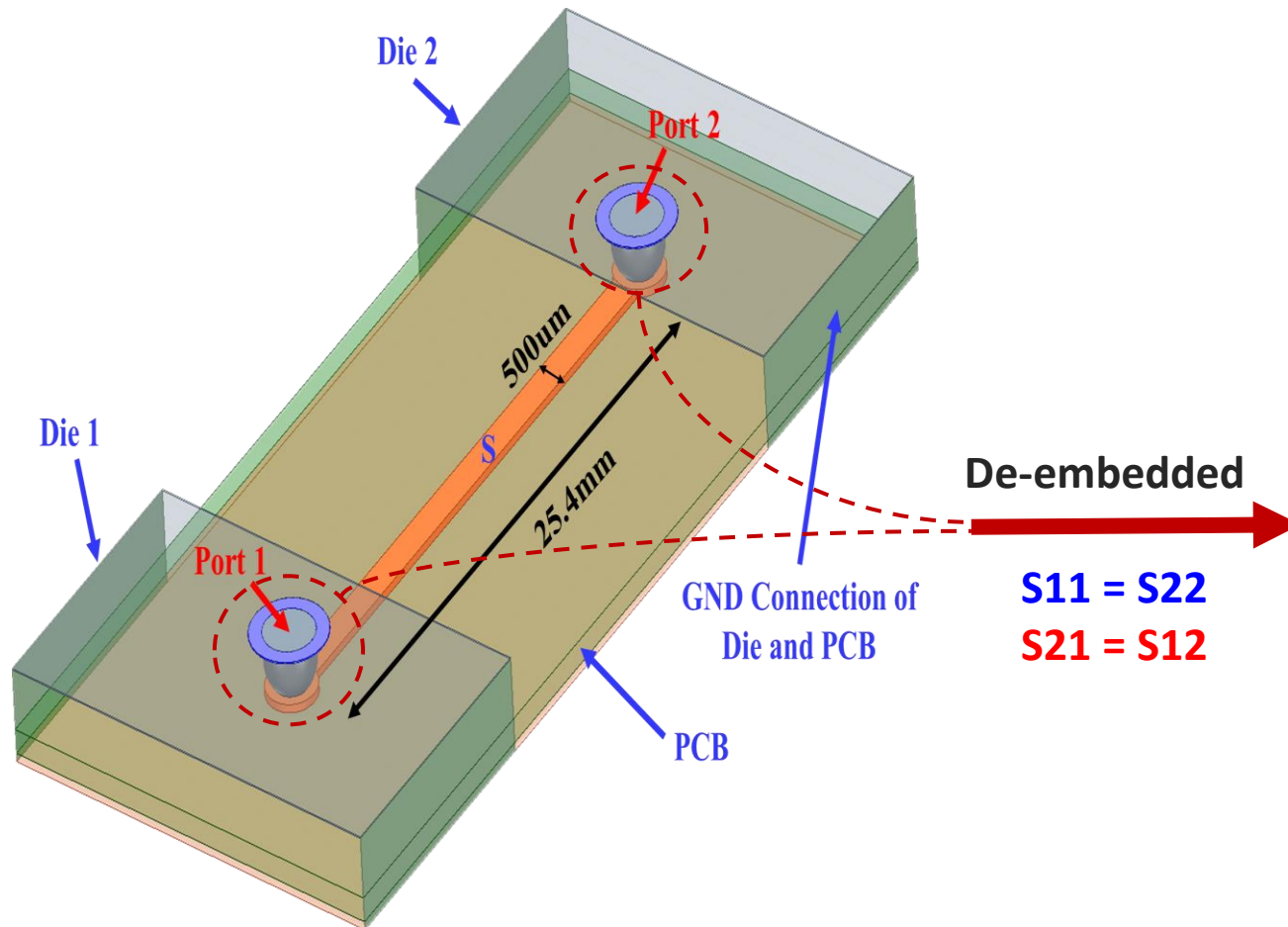
- L = 25.4mm → 10.65GHz
- L = 12.7mm → 14.25GHz
- L = 1.5mm → 18.8GHz



Characteristics impedance of L line

S-Parameter Extracted Bump By L-2L Method

22



Ref: Technical report, 2020 by Pouya Namaki and Nasser Masoumi

Electromagnetic Characteristics of Multiport TSVs Using L-2L De-Embedding Method and Shielding TSVs

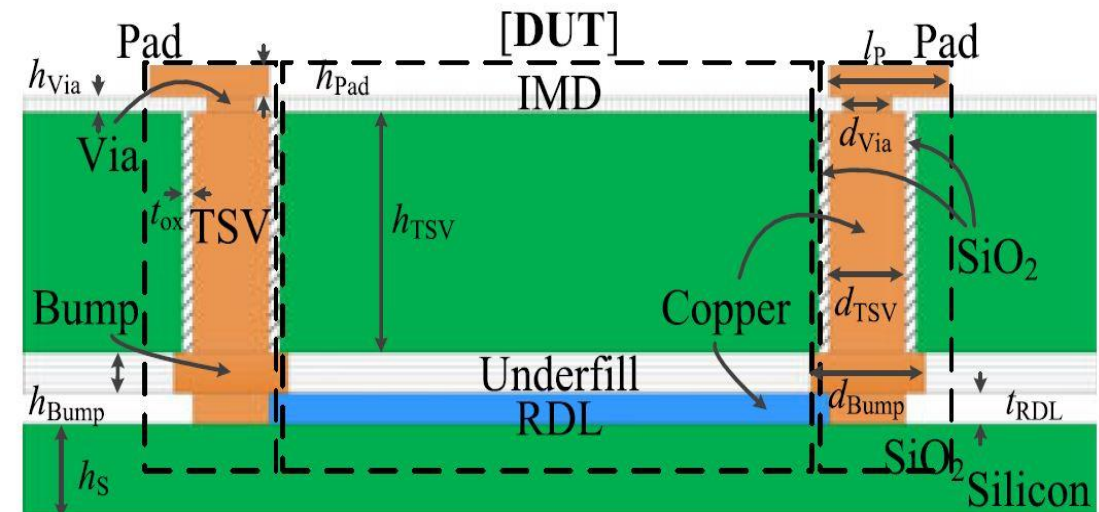
This paper presents: An L-2L de-embedding method for characterizing the electromagnetic properties of through silicon vias (TSVs) in 3-D ICs. (this is the first paper that discusses the use of de-embedding method for multiport TSVs.)

- Use of **L-2L** de-embedding method for **multiport TSVs**.
- **Proposed:** Modified structure.
- The performance of the designed structures **with and without shielding TSVs** is examined via both full-wave simulation and the measurements.

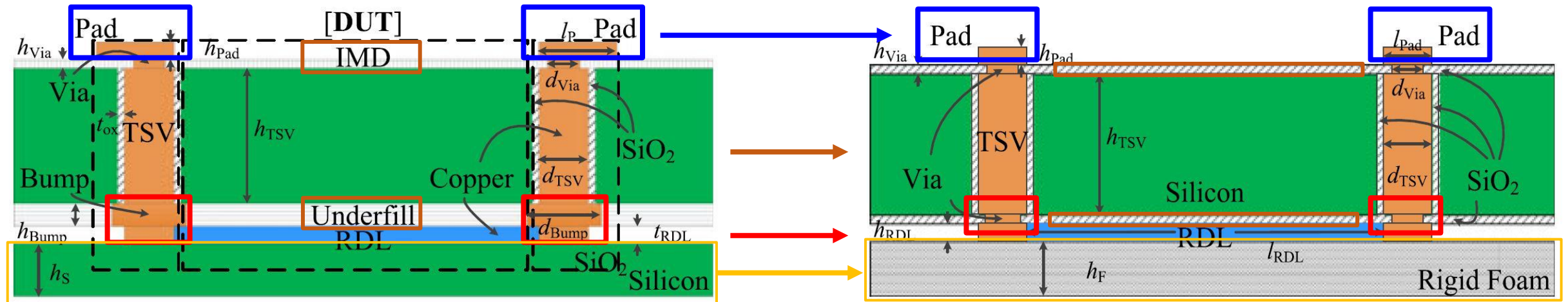
Authors: Yong-Sheng Li; Yan Li; Qiu Min; Ke Wu; En-Xiao Liu; Ran Hao; Hong-Sheng Chen; Cheng Zhuo; Wen-Yan Yin; Zhe-Yao, . . .

Journal: IEEE Transactions on Electromagnetic Compatibility.

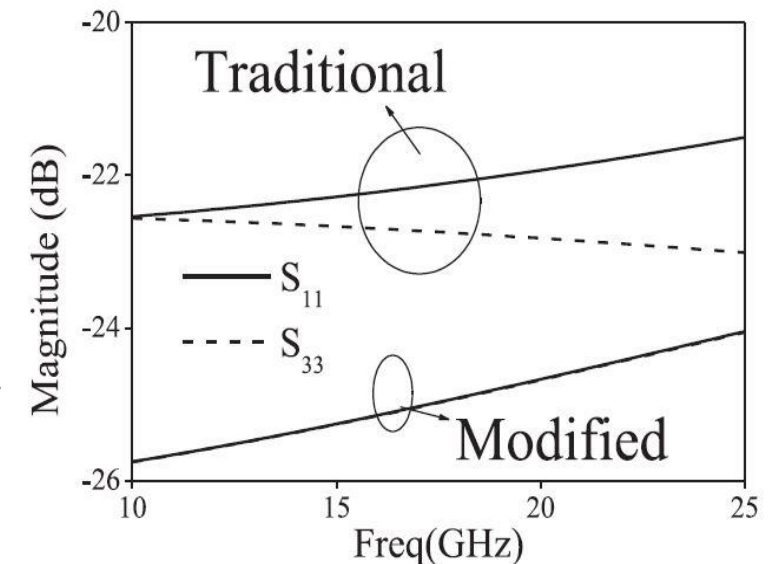
Date of publication: 15 march 2017



Traditional and Proposed Structures

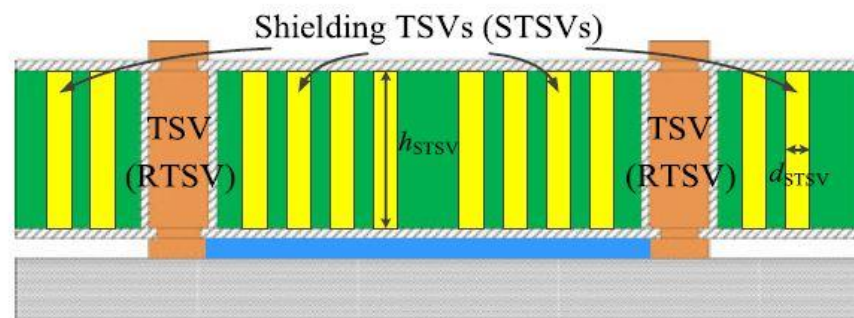


- **Pad**: The length of pads decreased
- **Between TSV and RDL**: **Bump** replaced by the **Via**
- **Substrate**: **Silicon** is change to a layer of **Rigid foam**
- **Insulation material**: The **insulation material** used in the **layer between pads** and the **silicon** and the **layer between the silicon and RDL** are chosen to be **SiO₂**.
- The **height of RDLs** is changed to be the same as that of the pads

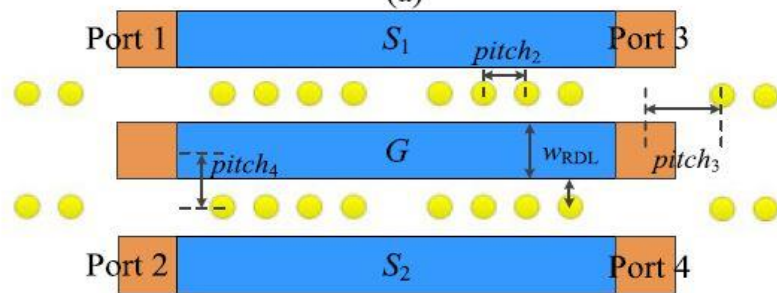


Structure with the Shielding TSVs

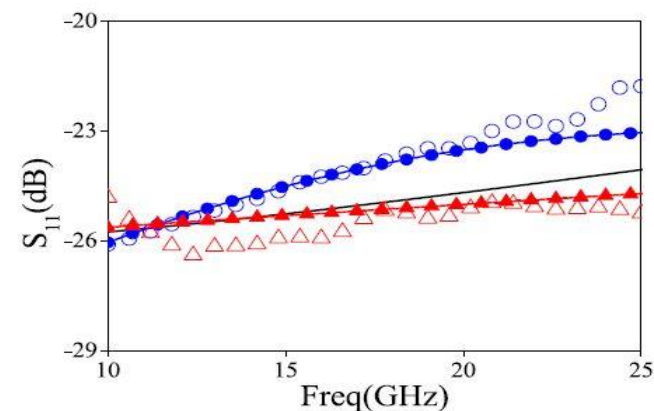
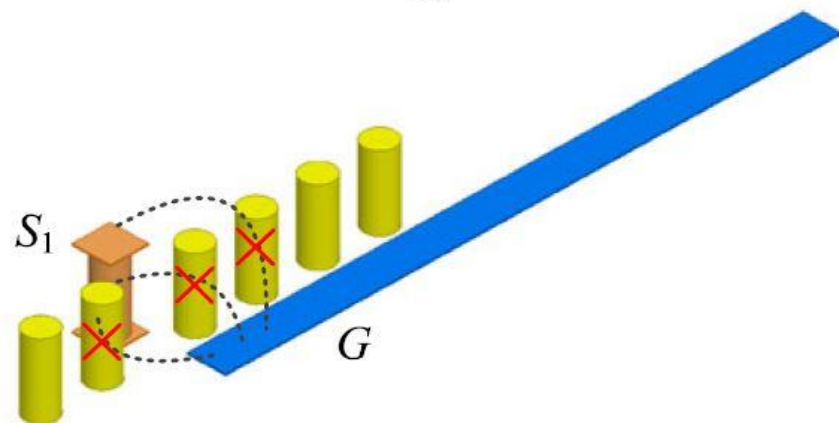
25



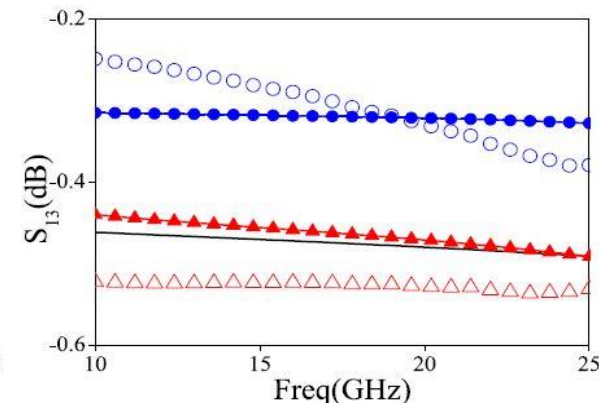
(a)



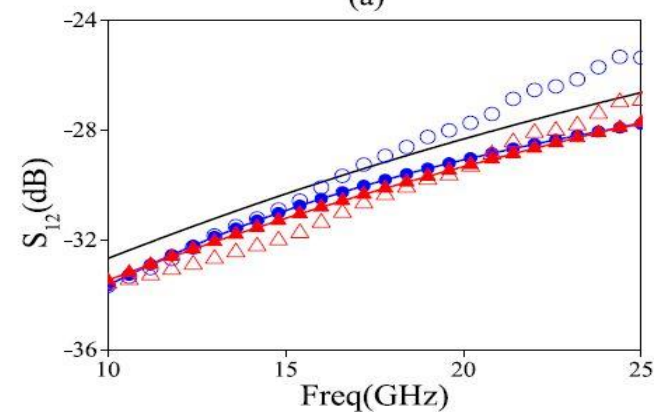
(b)



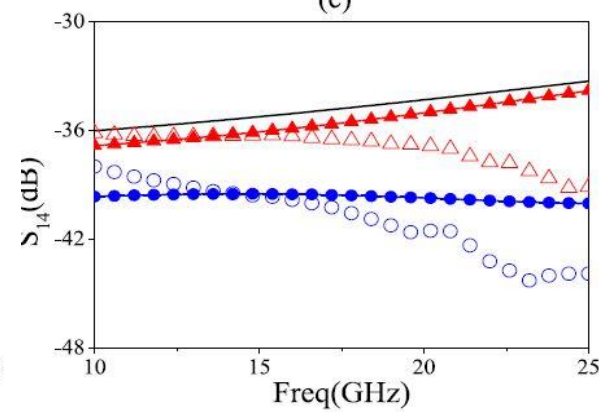
(a)



(c)



(d)

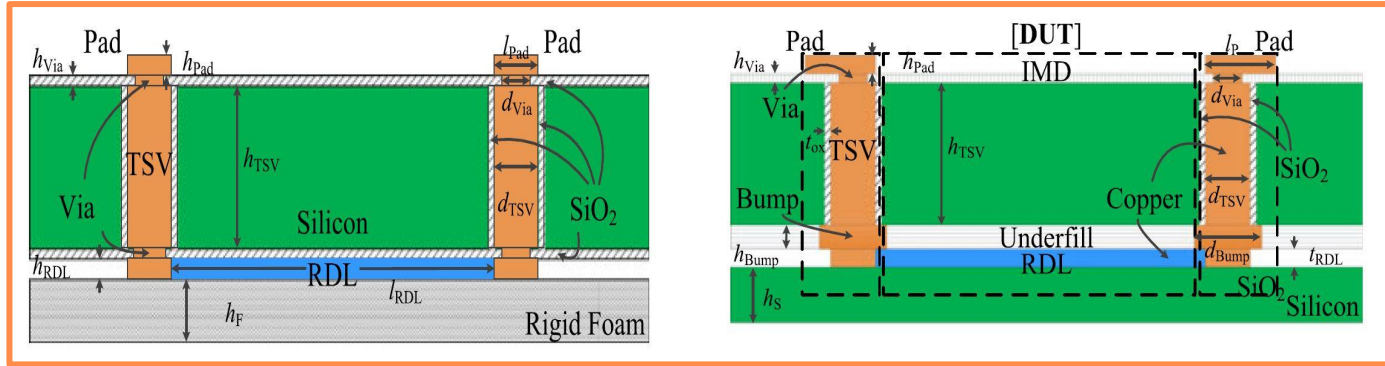


(e)

— Full-wave simulation of the SGS RTSVs

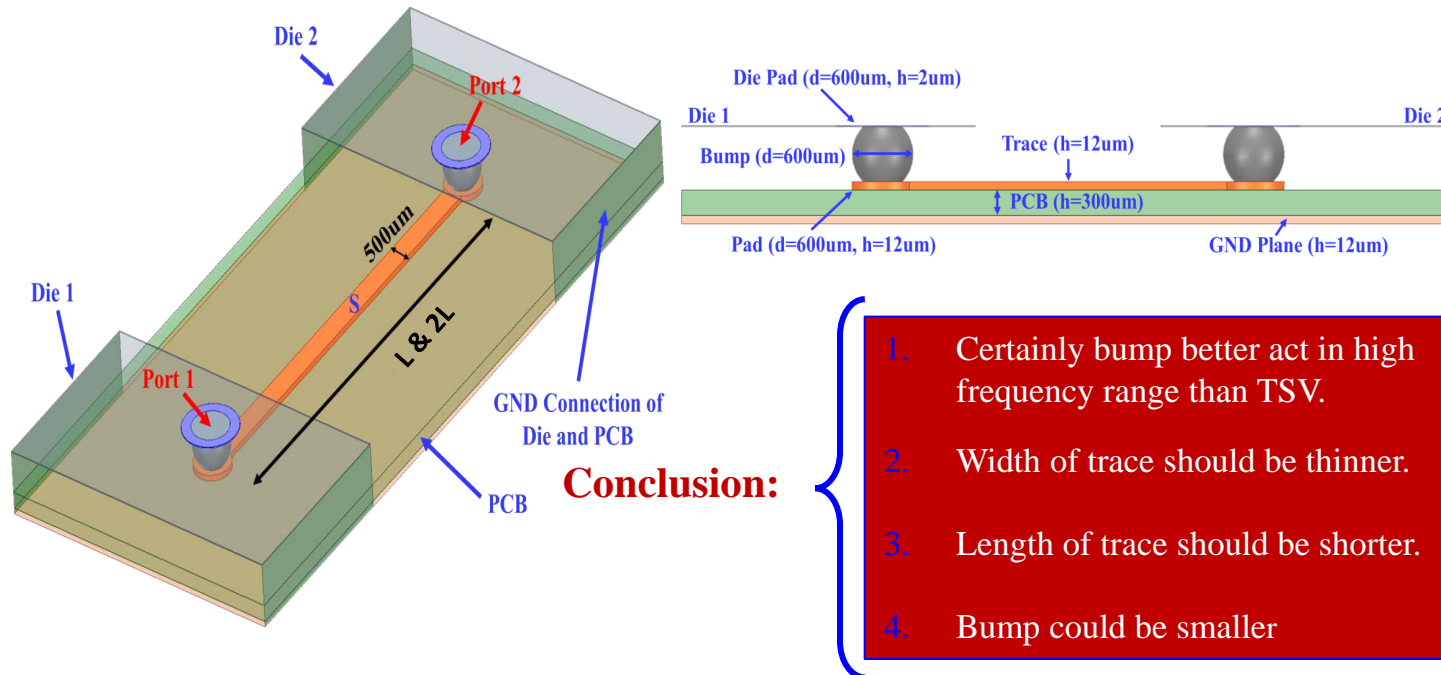
De-embedding results, w/o STSVs :	—●— Simulation	○ Measurement
De-embedding results, with STSVs :	—▲— Simulation	△ Measurement

Conclusion: Comparison to the Bump-Trace-Bump Structure



MATERIAL PARAMETERS AND DIMENSIONS

Design Parameter	Dimension	Material Parameter	Value
Pad thickness (h_{pad})	$2\ \mu\text{m}$	Conductivity of Si	10 S/m
Pad length (l_p)	$60\ \mu\text{m}$	Conductivity of copper	$5.95 \times 10^7\ \text{S/m}$
Pad length (l_{pad})	$50\ \mu\text{m}$	Conductivity of IMD	0 S/m
Via height (h_{via})	$0.5\ \mu\text{m}$	Conductivity of SiO ₂	0 S/m
Via diameter (d_{via})	$35\ \mu\text{m}$	Conductivity of Underfill	0 S/m
TSV height (h_{TSV})	$100\ \mu\text{m}$	Conductivity of Foam	0 S/m
TSV diameter (d_{TSV})	$40\ \mu\text{m}$	Relative permittivity of Si	11.9
Pitch between TSVs ($pitch_1$)	$100\ \mu\text{m}$	Relative permittivity of copper	1
Pitch between TSV and STSV ($pitch_2$)	$65\ \mu\text{m}$	Relative permittivity of IMD	1
Pitch between STSVs ($pitch_3$)	$80\ \mu\text{m}$	Relative permittivity of SiO ₂	4
Pitch between STSVs and RDL ($pitch_4$)	$50\ \mu\text{m}$	Relative permittivity of Underfill	1
SiO ₂ thickness (t_{ox})	$0.5\ \mu\text{m}$	Relative permittivity of Foam	1
Bump height (h_{bump})	$5\ \mu\text{m}$	Relative permeability of Si	1
Bump diameter (d_{bump})	$30\ \mu\text{m}$	Relative permeability of copper	1
RDL thickness (t_{RDL})	$1\ \mu\text{m}$	Relative permeability of IMD	1
RDL thickness (h_{RDL})	$2\ \mu\text{m}$	Relative permeability of SiO ₂	1
Substrate height (h_s)	$200\ \mu\text{m}$	Relative permeability of Underfill	1
Substrate height (h_F)	$5\ \text{mm}$	Relative permeability of Foam	1



Conclusion:

1. Certainly bump better act in high frequency range than TSV.
2. Width of trace should be thinner.
3. Length of trace should be shorter.
4. Bump could be smaller

✓ In high frequency range this method is accurate for **Die-interposer-Die** not for **Die-PCB –Die**.

- Use 2X Thru Method for Bump-Trace-Bump Structure
- Automatic Fixture Removal (AFR)
- Comparison of this methods

- [1] N. Erickson, K. Shringarpure, J. Fan, B. Achkir, S. Pan and C. Hwang, "De-embedding techniques for transmission lines: An exploration, review, and proposal," 2013 IEEE International Symposium on Electromagnetic Compatibility, Denver, CO, USA, 2013, pp. 840-845, doi: 10.1109/ISEMC.2013.6670527.
- [2] Ning LI, kota MATSUSHITA, Naok TAKAYAMA, Shogo ITO, Kenichi OKADA, Akira MATSUZAWA "Evaluation of a Multi-Line De-embedding Technique up to 110GHz for Millimeter-Wave CMOS Circuit Design" 2010 IEICE Transactions on Fundamentals of Electronics Communications and Computer Sciences 93-A(2):431-439
- [3] Y. Chang, S. S. H. Hsu, D. Chang, J. Lee, S. Lin and Y. Juang, "A de-embedding method for extracting S-parameters of vertical interconnect in advanced packaging," 2011 IEEE 20th Conference on Electrical Performance of Electronic Packaging and Systems, San Jose, CA, USA, 2011, pp. 219-222, doi: 10.1109/EPEPS.2011.6100231.
- [4] A. M. Mangan, S. P. Voinigescu, Ming-Ta Yang and M. Tazlauanu, "De-embedding transmission line measurements for accurate modeling of IC designs," in IEEE Transactions on Electron Devices, vol. 53, no. 2, pp. 235-241, Feb. 2006, doi: 10.1109/TED.2005.861726.
- [5] Qing-Hong Bu, Ning Li, Keigo Bunsen, Hiroki Asada, Kota Matsushita, "Evaluation of a Multi-line De-embedding Technique for Millimeter-Wave CMOS Circuit Design" Proceeding of Asia-Pacific Microwave Conference 2010
- [6] G. F. Engen and C. A. Hoer, "Thru-Reflect-Line: An Improved Technique for Calibrating the Dual Six-Port Automatic Network Analyzer," in IEEE Transactions on Microwave Theory and Techniques, vol. 27, no. 12, pp. 987-993, Dec. 1979, doi: 10.1109/TMTT.1979.1129778.
- [7] P. Colestock and M. Foley, "A Generalized TRL Algorithm for S-Parameter De-Embedding", Fermi National Accelerator Laboratory, April 1993
- [8] Chen, Yuan, "De-embedding method comparisons and physics based circuit model for high frequency D-probe" (2018). Masters Theses. 7757.
- [10] J. Hanning, J. Stenarson, K. Yhland, P. J. Sobis, T. Bryllert and J. Stake, "Single-Flange 2-Port TRL Calibration for Accurate THz S -Parameter Measurements of Waveguide Integrated Circuits," in IEEE Transactions on Terahertz Science and Technology, vol. 4, no. 5, pp. 582-587, Sept. 2014, doi: 10.1109/TTHZ.2014.2342497
- [11] C. Wu, B. Chen, T. Mikheil, J. Fan and X. Ye, "Error bounds analysis of de-embedded results in 2x thru de-embedding methods," 2017 IEEE International Symposium on Electromagnetic Compatibility & Signal/Power Integrity (EMCSI), 2017, pp. 532-536, doi: 10.1109/ISEMC.2017.8077927.
- [12] Bichen Chen "2X-Thru, 1X-Reflection, and Thru-Line de-embedding: Theory, sensitivity analysis, and error corrections"(2019). Phd Theses.
- [13] DesignCon, "A NIST Traceable PCB Kit for Evaluating the Accuracy of De-Embedding Algorithms and Corresponding Metrics" 2018
- [14] H. Cho, J. Huang, C. Kuo, S. Liu and C. Wu, "A Novel Transmission-Line Deembedding Technique for RF Device Characterization," in IEEE Transactions on Electron Devices, vol. 56, no. 12, pp. 3160-3167, Dec. 2009, doi: 10.1109/TED.2009.2032608.
- [15] Ning Li, "Evaluation of a Multi-Line De-Embedding Technique up to 110 GHz for Millimeter-Wave CMOS Circuit Design", February 2010 IEICE Transactions on Fundamentals of Electronics Communications and Computer Sciences 93-A(2):431-439
- [16] Y. -S. Li et al., "Electromagnetic Characteristics of Multiport TSVs Using L-2L De-Embedding Method and Shielding TSVs," in IEEE Transactions on Electromagnetic Compatibility, vol. 59, no. 5, pp. 1541-1548, Oct. 2017, doi: 10.1109/TEMC.2017.2664047.
- [17] A. Usman et al., "Interposer Technologies for High-Performance Applications," in IEEE Transactions on Components, Packaging and Manufacturing Technology, vol. 7, no. 6, pp. 819-828, June 2017, doi: 10.1109/TCPMT.2017.2674686.